bile/BC structures. There might be aberrant fucose overloading of the sorting machinery in HepG2 cells because the numbers of BC structures of HepG2 cells are limited. We also reported that AFP had several kinds of alpha1−6 fucosylated structures, although the percentages were small.[4] Comparison of oligosaccharide structures on AFP derived from the BC structures with the conditioned medium is our greatest interest, although the analysis is impossible because of low levels of AFP in the BC structures.

Characters of human hepatoblastoma, HepG2 cells, correspond to neither HCCs nor normal hepatocytes. It has been reported that a number of cell lines, such as Huh7 cells and WIF-B9 cells, can form BC structures.[29] However, we were unable to obtain a sufficient amount of protein from the BC structures of cells other than HepG2. The numbers of BC structures in the other cell lines examined were much lower than those in HepG2 under our culture conditions. Therefore, our data in the present study might be limited in HepG2 cells. It is well accepted that the secretory pathway is dramatically changed in many cases in cancers and especially in HCC. To know whether or not increases of fucosylated AFP (AFP-L3) in sera of patients with HCC are dependent on the abnormality of the secretory pathway of fucosylated glycoproteins, a study using much more human liver tissues bearing HCC should be performed. Another possibility is that an abnormality of fucose-specific lectin in the liver, if it exits, is induced in HCC tissues.

Early detection of HCC is essential for successful treatment. The recent development of highly sensitive detection systems for AFP-L3 enables us to detect HCC at an early stage.[26,30] On the other hand, increased fucosylation in sera of HCC patients are not limited to AFP. There are many reports that increases in the levels of fucosylation of serum glycoproteins occur with the development of HCC.[31−33] Clarification of the mechanism underlying the polarized secretion of fucosylated glycoproteins in the liver will lead to the development of novel glyco-cancer biomarkers.

AUTHOR INFORMATION

Corresponding Author

*Tel: +81-6-6879-2590. Fax: +81-6-6879-2590. E-mail: emiyoshi@sahs.med.osaka-u.ac.jp.

Notes

The authors declare no competing financial interest.

ACKNOWLEDGMENTS

This work was supported by the New Energy and Industrial Technology Development Organization (NEDO) as a part of the Developing Technology Project for Implementing Sugar Chain Functions in Japan. This work was also supported in part by the Global COE Program of Osaka University funded by the Ministry of Education, Culture, Sports, Science, and Technology of Japan and a Grant-in-Aid for Scientific Research (A), No. 21249038, from the Japan Society for the Promotion of Science.

ABBREVIATIONS

AFP-L3, L3 fraction of alpha-fetoprotein; HCC, hepatocellular carcinoma; Fut8, alpha1−6 fucosyltransferase; FX, human homologue of GDP-4-keto-6-deoxymannose-3,5-epimerase-4-reductase; BC, bile canaliculus; GMD, GDP-mannose-4,6-dehydratase; AOL, *Aspergillus oryzae* lectin; FBS, fetal bovine serum; DKD, double knock-down; shRNA, small hairpin RNA; SDS-PAGE, sodium dodecylsulfate-polyacrylamide gel electrophoresis; TBS, Tris-buffered saline; TBST, TBS containing 0.05% Tween 20; LCA, *Lens culinaris*; PA, pyridylamino; HPLC, high-performance liquid chromatography; LC-ESI-MS/MS, liquid chromatography-electrospray ionization-tandem mass spectrometry; AGP, alpha1-acid glycoprotein

REFERENCES

(1) Morinaga, T.; Sakai, M.; Wegmann, T. G.; Tamaoki, T. Primary structures of human alpha-fetoprotein and its mRNA. *Proc. Natl. Acad. Sci. U. S. A.* **1983**, *80* (15), 4604−8.

(2) Yoshima, H.; Mizuochi, T.; Ishii, M.; Kobata, A. Structure of the asparagine-linked sugar chains of alpha-fetoprotein purified from human ascites fluid. *Cancer Res.* **1980**, *40* (11), 4276−81.

(3) Yamashita, K.; Taketa, K.; Nishi, S.; Fukushima, K.; Ohkura, T. Sugar chains of human cord serum alpha-fetoprotein: characteristics of *N*-linked sugar chains of glycoproteins produced in human liver and hepatocellular carcinomas. *Cancer Res.* **1993**, *53* (13), 2970−5.

(4) Nakagawa, T.; Miyoshi, E.; Yakushijin, T.; Hiramatsu, N.; Igura, T.; Hayashi, N.; Taniguchi, N.; Kondo, A. Glycomic analysis of alpha-fetoprotein L3 in hepatoma cell lines and hepatocellular carcinoma patients. *J. Proteome Res.* **2008**, *7* (6), 2222−33.

(5) Taketa, K. Alpha-fetoprotein: reevaluation in hepatology. *Hepatology* **1990**, *12* (6), 1420−32.

(6) Uozumi, N.; Yanagidani, S.; Miyoshi, E.; Ihara, Y.; Sakuma, T.; Gao, C. X.; Teshima, T.; Fujii, S.; Shiba, T.; Taniguchi, N. Purification and cDNA cloning of porcine brain GDP-L-Fuc:*N*-acetyl-beta-D-glucosaminide alpha1−6fucosyltransferase. *J. Biol. Chem.* **1996**, *271* (44), 27810−7.

(7) Yanagidani, S.; Uozumi, N.; Ihara, Y.; Miyoshi, E.; Yamaguchi, N.; Taniguchi, N. Purification and cDNA cloning of GDP-L-Fuc:*N*-acetyl-beta-D-glucosaminide:alpha1−6 fucosyltransferase (alpha1−6 FucT) from human gastric cancer MKN45 cells. *J. Biochem.* **1997**, *121* (3), 626−32.

(8) Noda, K.; Miyoshi, E.; Uozumi, N.; Yanagidani, S.; Ikeda, Y.; Gao, C.; Suzuki, K.; Yoshihara, H.; Yoshikawa, K.; Kawano, K.; Hayashi, N.; Hori, M.; Taniguchi, N. Gene expression of alpha1−6 fucosyltransferase in human hepatoma tissues: a possible implication for increased fucosylation of alpha-fetoprotein. *Hepatology* **1998**, *28* (4), 944−52.

(9) Noda, K.; Miyoshi, E.; Nakahara, S.; Ihara, H.; Gao, C. X.; Honke, K.; Yanagidani, S.; Sasaki, Y.; Kasahara, A.; Hori, M.; Hayashi, N.; Taniguchi, N. An enzymatic method of analysis for GDP-L-fucose in biological samples, involving high-performance liquid chromatography. *Anal. Biochem.* **2002**, *310* (1), 100−6.

(10) Noda, K.; Miyoshi, E.; Gu, J.; Gao, C. X.; Nakahara, S.; Kitada, T.; Honke, K.; Suzuki, K.; Yoshihara, H.; Yoshikawa, K.; Kawano, K.; Tonetti, M.; Kasahara, A.; Hori, M.; Hayashi, N.; Taniguchi, N. Relationship between elevated FX expression and increased production of GDP-L-fucose, a common donor substrate for fucosylation in human hepatocellular carcinoma and hepatoma cell lines. *Cancer Res.* **2003**, *63* (19), 6282−9.

(11) Tonetti, M.; Sturla, L.; Bisso, A.; Benatti, U.; De Flora, A. Synthesis of GDP-L-fucose by the human FX protein. *J. Biol. Chem.* **1996**, *271* (44), 27274−9.

(12) Kristiansen, T. Z.; Bunkenborg, J.; Gronborg, M.; Molina, H.; Thuluvath, P. J.; Argani, P.; Goggins, M. G.; Maitra, A.; Pandey, A. A proteomic analysis of human bile. *Mol. Cell. Proteomics* **2004**, *3* (7), 715−28.

(13) Nakagawa, T.; Uozumi, N.; Nakano, M.; Mizuno-Horikawa, Y.; Okuyama, N.; Taguchi, T.; Gu, J.; Kondo, A.; Taniguchi, N.; Miyoshi, E. Fucosylation of *N*-glycans regulates the secretion of hepatic glycoproteins into bile ducts. *J. Biol. Chem.* **2006**, *281* (40), 29797−806.

(14) Nakagawa, T.; Takeishi, S.; Kameyama, A.; Yagi, H.; Yoshioka, T.; Moriwaki, K.; Masuda, T.; Matsumoto, H.; Kato, K.; Narimatsu, H.; Taniguchi, N.; Miyoshi, E. Glycomic analyses of glycoproteins in

bile and serum during rat hepatocarcinogenesis. *J. Proteome Res.* **2010**, *9* (10), 4888–96.
(15) Sormunen, R.; Eskelinen, S.; Lehto, V. P. Bile canaliculus formation in cultured HEPG2 cells. *Lab. Invest.* **1993**, *68* (6), 652–62.
(16) van, I. S. C.; Hoekstra, D. Polarized sphingolipid transport from the subapical compartment changes during cell polarity development. *Mol. Biol. Cell* **2000**, *11* (3), 1093–101.
(17) Zegers, M. M.; Hoekstra, D. Mechanisms and functional features of polarized membrane traffic in epithelial and hepatic cells. *Biochem. J.* **1998**, *336* (Pt 2), 257–69.
(18) Bastaki, M.; Braiterman, L. T.; Johns, D. C.; Chen, Y. H.; Hubbard, A. L. Absence of direct delivery for single transmembrane apical proteins or their "Secretory" forms in polarized hepatic cells. *Mol. Biol. Cell* **2002**, *13* (1), 225–37.
(19) Miyoshi, E.; Ihara, Y.; Hayashi, N.; Fusamoto, H.; Kamada, T.; Taniguchi, N. Transfection of *N*-acetylglucosaminyltransferase III gene suppresses expression of hepatitis B virus in a human hepatoma cell line, HB611. *J. Biol. Chem.* **1995**, *270* (47), 28311–5.
(20) Tomiya, N.; Awaya, J.; Kurono, M.; Endo, S.; Arata, Y.; Takahashi, N. Analyses of *N*-linked oligosaccharides using a two-dimensional mapping technique. *Anal. Biochem.* **1988**, *171* (1), 73–90.
(21) Takahashi, N.; Kato, K. GALAXY (glycoanalysis by the three axes of MS and chromatography): a web application that assists structural analyses of *N*-glycans. *Trends Glycosci. Glycotechnol.* **2003**, *15* (84), 235–51.
(22) Misonou, Y.; Shida, K.; Korekane, H.; Seki, Y.; Noura, S.; Ohue, M.; Miyamoto, Y. Comprehensive clinico-glycomic study of 16 colorectal cancer specimens: elucidation of aberrant glycosylation and its mechanistic causes in colorectal cancer cells. *J. Proteome Res.* **2009**, *8* (6), 2990–3005.
(23) Tateno, H.; Nakamura-Tsuruta, S.; Hirabayashi, J. Comparative analysis of core-fucose-binding lectins from *Lens culinaris* and *Pisum sativum* using frontal affinity chromatography. *Glycobiology* **2009**, *19* (5), 527–36.
(24) Becker, D. J.; Lowe, J. B. Fucose: biosynthesis and biological function in mammals. *Glycobiology* **2003**, *13* (7), 41R–53R.
(25) Kuno, A.; Ikehara, Y.; Tanaka, Y.; Angata, T.; Unno, S.; Sogabe, M.; Ozaki, H.; Ito, K.; Hirabayashi, J.; Mizokami, M.; Narimatsu, H. Multilectin assay for detecting fibrosis-specific glyco-alteration by means of lectin microarray. *Clin. Chem.* **2011**, *57* (1), 48–56.
(26) Hanaoka, T.; Sato, S.; Tobita, H.; Miyake, T.; Ishihara, S.; Akagi, S.; Amano, Y.; Kinoshita, Y. Clinical significance of the highly sensitive fucosylated fraction of alpha-fetoprotein in patients with chronic liver disease. *J. Gastroenterol. Hepatol.* **2011**, *26* (4), 739–44.
(27) Kitagawa, Y.; Sano, Y.; Ueda, M.; Higashio, K.; Narita, H.; Okano, M.; Matsumoto, S.; Sasaki, R. *N*-Glycosylation of erythropoietin is critical for apical secretion by Madin-Darby canine kidney cells. *Exp. Cell Res.* **1994**, *213* (2), 449–57.
(28) Comunale, M. A.; Rodemich-Betesh, L.; Hafner, J.; Wang, M.; Norton, P.; Di Bisceglie, A. M.; Block, T.; Mehta, A. Linkage specific fucosylation of alpha-1-antitrypsin in liver cirrhosis and cancer patients: implications for a biomarker of hepatocellular carcinoma. *PLoS One* **2010**, *5* (8), e12419.
(29) Decaens, C.; Durand, M.; Grosse, B.; Cassio, D. Which in vitro models could be best used to study hepatocyte polarity? *Biol. Cell* **2008**, *100* (7), 387–98.
(30) Tamura, Y.; Igarashi, M.; Kawai, H.; Suda, T.; Satomura, S.; Aoyagi, Y. Clinical advantage of highly sensitive on-chip immunoassay for fucosylated fraction of alpha-fetoprotein in patients with hepatocellular carcinoma. *Dig. Dis. Sci.* **2010**, *55* (12), 3576–83.
(31) Block, T. M.; Comunale, M. A.; Lowman, M.; Steel, L. F.; Romano, P. R.; Fimmel, C.; Tennant, B. C.; London, W. T.; Evans, A. A.; Blumberg, B. S.; Dwek, R. A.; Mattu, T. S.; Mehta, A. S. Use of targeted glycoproteomics to identify serum glycoproteins that correlate with liver cancer in woodchucks and humans. *Proc. Natl. Acad. Sci. U. S. A.* **2005**, *102* (3), 779–84.
(32) Comunale, M. A.; Lowman, M.; Long, R. E.; Krakover, J.; Philip, R.; Seeholzer, S.; Evans, A. A.; Hann, H. W.; Block, T. M.; Mehta, A. S. Proteomic analysis of serum associated fucosylated glycoproteins in the development of primary hepatocellular carcinoma. *J. Proteome Res.* **2006**, *5* (2), 308–15.
(33) Comunale, M. A.; Wang, M.; Hafner, J.; Krakover, J.; Rodemich, L.; Kopenhaver, B.; Long, R. E.; Junaidi, O.; Bisceglie, A. M.; Block, T. M.; Mehta, A. S. Identification and development of fucosylated glycoproteins as biomarkers of primary hepatocellular carcinoma. *J. Proteome Res.* **2009**, *8* (2), 595–602.

DOI: 10.1111/j.1600-0625.2012.01515.x
www.blackwellpublishing.com/EXD

Original Article

Upregulation of *N*-acetylglucosaminyltransferase-V by heparin-binding EGF-like growth factor induces keratinocyte proliferation and epidermal hyperplasia

Akihiro Kimura[1,2]*, Mika Terao[1,2]*, Arisa Kato[1,2], Takaaki Hanafusa[2], Hiroyuki Murota[2], Ichiro Katayama[2] and Eiji Miyoshi[1]

[1]Department of Molecular Biochemistry and Clinical Investigation, Osaka University Graduate School of Medicine, Suita, Japan; [2]Department of Dermatology, Osaka University Graduate School of Medicine, Suita, Japan

Correspondence: Eiji Miyoshi, Department of Molecular Biochemistry and Clinical Investigation, 1-7, Yamada-oka, Suita 565-0871, Japan, Tel.: +81-6-6879-2590, Fax: + 81-6-6879-2590, e-mail: emiyoshi@sahs.med.osaka-u.ac.jp

**These authors equally contribute to this work.*

Abstract: Oligosaccharide modification by *N*-acetylglucosaminyltransferase-V (GnT-V), a glycosyltransferase encoded by the *Mgat5* gene that catalyses the formation of β1,6 GlcNAc (*N*-acetylglucosamine) branches on *N*-glycans, is thought to be associated with cancer growth and metastasis. Overexpression of GnT-V in cancer cells enhances the signalling of growth factors such as epidermal growth factor (EGF) and transforming growth factor-β by increasing galectin-3 binding to polylactosamine structures on receptor *N*-glycans. We previously demonstrated that transgenic mice overexpressing GnT-V fail to develop spontaneous tumors in any organs, but phenotypes reminiscent of epithelial-to-mesenchymal transition were observed in their skin. However, the biological function of GnT-V in normal skin remained unknown. In this study, we examined the role of GnT-V in keratinocyte proliferation using GnT-V-deficient mice. Proliferation of human keratinocytes was suppressed by treatment with GnT-V siRNA. *Mgat5*$^{-/-}$ mouse keratinocytes also showed impaired cell proliferation through the reduction in EGF receptors on the cell surface. Although the skin of *Mgat5*$^{-/-}$ mice appeared normal, epidermal hyperplasia and proliferation of keratinocytes induced by the phorbol ester 12-O-tetradecanoyl phorbol-13-acetate (TPA) were downregulated in these mutants. Moreover, a dramatic increase in GnT-V expression was observed by treatment with TPA or heparin-binding EGF-like growth factor (HB-EGF) in normal human epidermal keratinocytes. This increase was inhibited by an EGF receptor inhibitor. These results indicate that a high expression of GnT-V in keratinocytes contributes to HB-EGF-mediated epidermal hyperproliferation by inhibiting endocytosis of EGF receptors bearing β1,6 GlcNAc on their *N*-glycans. Our findings demonstrate a novel role for GnT-V in epidermal homoeostasis, particularly in hyperproliferative conditions.

Abbreviation: GnT-V, *N*-acetylglucosaminyltransferase-V; GlcNAc, *N*-acetylglucosamine; EGF, epidermal growth factor; EGFR, epidermal growth factor receptor; HB-EGF, heparin-binding epidermal growth factor-like growth factor; NHEK, normal human epidermal keratinocyte; TPA, phorbol ester 12-O-tetradecanoyl phorbol-13-acetate; *Mgat5*$^{-/-}$ mouse, *N*-acetylglucosaminyltransferase-V knockout mouse.

Key words: glycosylation – GnT-V – HB-EGF – hyperproliferation – keratinocytes

Accepted for publication 25 April 2012

Introduction

Glycans are oligosaccharides that are attached to proteins via two major linkage types, *N*-glycans and *O*-glycans. Changes in glycosylation are observed during differentiation and carcinogenesis (1) and are regulated by a series of glycosyltransferases. *N*-acetylglucosaminyltransferase-V (GnT-V), a glycosyltransferase encoded by the *Mgat5* gene, is known to play an important role in tumor growth and metastasis (2, 3). Our previous study demonstrated that GnT-V expression is associated with poor disease prognosis, as judged by immunohistochemical analysis (3, 4). In addition, mammary tumor growth and metastasis induced by the polyomavirus middle T oncogene is considerably reduced in *N*-acetylglucosaminyltransferase-V knockout mice (*Mgat5*$^{-/-}$ mice) compared to littermate controls (5). We recently reported that GnT-V transgenic mouse keratinocytes exhibit epithelial-to-mesenchymal transition-like phenotype and promote wound healing (6). Besides its association with tumor growth, GnT-V expression is increased in the regenerating rat liver (7).

GnT-V catalyses the formation of β1-6 GlcNAc branches on *N*-glycans, allowing for the formation of polylactosamines. The resultant oligosaccharide structure can associate with galectin-3 to form a molecular lattice that prevents glycoprotein endocytosis, leaving the activated receptors at the cell surface, where they promote signalling and cell growth. In GnT-V-deficient mammary tumor cells from *Mgat5*$^{-/-}$ mice, epidermal growth factor receptor (EGFR) signalling is reduced through decreased galectin-3 binding to polylactosamines and rapid internalization of EGFR from the cell surface (8). In addition, mammary tumor cells from *Mgat5*$^{-/-}$ mice are insensitive to epidermal growth factor (EGF), fibroblast growth factor and transforming growth factor-β (9). Downregulation of β1,6 GlcNAc branching by overexpression of GnT-III (*N*-acetylglucosaminyltransferase-III), which antagonizes GnT-V activity through conformational changes in *N*-glycans (10), also decreases EGFR signalling (11). These reports highlight the importance of GnT-mediated glycosylation of EGFR for tumor cell function.

Epidermal growth factor receptor-mediated signalling also plays a crucial role in maintaining homoeostasis in the skin. The proliferation of mature, healthy epidermal cells is maintained by balancing signalling from various EGF family members, such as heparin-binding epidermal growth factor-like growth factor (HB-EGF), transforming growth factor-α and amphiregulin, all of which bind to EGFR in the epidermis (12–14). Given that aberrant glycosylation by GnT-V is reported to modulate EGFR signalling and that overproliferation of keratinocytes causes epidermal hyperplasia, we hypothesized that GnT-V is involved in keratinocyte proliferation and epidermal hyperplasia.

To address this possibility, we examined the proliferation of normal human epidermal keratinocytes (NHEKs) and *Mgat5*$^{-/-}$ mouse keratinocytes under several conditions. We found that HB-EGF-induced proliferation of keratinocytes was mediated by the upregulation of GnT-V expression. Moreover, the *Mgat5*$^{-/-}$ mouse epidermis was resistant to hyperproliferative stimuli. Our data suggest that HB-EGF induces keratinocyte proliferation through two pathways: direct stimulation of EGFR and stabilization of cell surface EGFR expression via GnT-V-mediated glycosylation.

Material and methods

Cell culture

A normal human epidermal keratinocytes (NHEKs) cell lines were purchased from DS Pharma Biomedical (Osaka, Japan). NHEKs were cultured on type-1 collagen-coated plates (Asahi Techno Glass, Funabashi, Japan) in human keratinocyte serum-free medium (DS Pharma Biomedical, Osaka, Japan) supplemented with bovine pituitary extract.

Isolation and culture of mouse keratinocytes were carried out as previously described (15). Full-thickness skin harvested from day 2 to day 4 newborn mice or 12-week-old mouse tail was treated with 4 mg/ml of dispase (Gibco; Invitrogen, Paisley, UK) for 1 h at 37°C. Next, the epidermis was peeled from the dermis. The epidermis was trypsinized to prepare single cells. It was then incubated in human keratinocyte serum-free medium for 6 h at 37°C under an atmosphere with 5% CO_2. Non-adherent cells were washed away with phosphate-buffered saline (PBS) twice, and then cultured for 2–3 days in human keratinocyte serum-free medium before use in experiments.

The cells were treated with EGFR inhibitor, AG1478 (LC Laboratories, Woburn, MA, USA), HB-EGF (R&D Systems, Minneapolis, MN, USA) and EGF (R&D Systems) in some experiments.

Mice

Mgat5$^{-/-}$ mice on a C57BL/6 background were obtained from The Jackson Laboratory, Inc (Bar Harbor, ME, USA). Animal care was in accordance with the institutional guidelines of Osaka University. All of the animal experiments were carried out with the approval of the Animal Experiments Committee of Osaka University (#20-003-0).

Histopathological analysis

Harvested skin samples were fixed in 10% formaldehyde for 24 h, followed by embedding in paraffin and microtome sectioning. Slides were stained with haematoxylin and eosin (H&E). For immunohistochemical analysis, sections were hydrated by passage through xylene and graded ethanols. After antigen retrieval for 10 min at 90°C in citric buffer, pH 6.0, the slides were blocked with serum-free protein block (Dako-Cytomation, Carpinteria, CA, USA) for 10 min, then incubated with primary antibody overnight at 4°C (rabbit anti-Ki-67 antibody 1:500 dilution, Novocastra Laboratories Ltd, Newcastle, UK). After washing with tris-buffered saline (TBS) containing 0.05% Triton-X100, slides were mounted using the Vectastain ABC kit® (Vector Laboratories, Burlingame, CA, USA) followed by counterstaining with haematoxylin. Rabbit IgG were used as the isotype controls.

Immunofluorescence Staining of Keratinocytes

Mouse keratinocytes were isolated as described earlier, seeded into dishes precoated with type-1 collagen (6×10^5 cells/ml) and grown to confluence. Cells were fixed with 4% paraformaldehyde. The cells were then incubated with the primary antibody, rabbit anti-EGF receptor (1:1000 dilution; Cell Signaling Technology Inc, Beverly, MA, USA), followed by the secondary antibody (anti-rabbit Alexa Fluor 488; Invitrogen). Hoechst 33342 was used to stain nucleus. The cells were visualized using a Keyence Biozero confocal microscope (Keyence co., Osaka, Japan).

Western blot analysis

Cell samples were solubilized at 4°C in lysis buffer (0.5% sodium deoxycholate, 1% Nonidet P40, 0.1% sodium dodecylsulphate, 100 μg/ml phenylmethylsulphonyl fluoride, 1 mM sodium orthovanadate and protease inhibitor cocktail). A cellular membrane fraction was prepared with Mem-PER (Thermo Scientific, Rockford, IL, USA), according to the manufacturer's instructions. Same amount of proteins (30 μg) were separated on SDS-polyacrylamide gels and transferred onto polyvinylidine fluoride membranes (Bio-Rad, Hercules, CA, USA). Non-specific protein binding was blocked by incubating the membranes in 5% w/v non-fat milk powder in TBS-T (50 mM Tris–HCl, pH 7.6, 150 mM NaCl and 0.1% v/v Tween 20). The membranes were incubated with rabbit anti-EGF receptor antibody (Cell Signaling Technology), rabbit anti-phospho-EGF receptor antibody (Cell Signaling Technology), rabbit anti-p44/42 MAP Kinase antibody (Cell Signaling Technology), rabbit anti-phospho-p44/42 MAPK antibody (Cell Signaling Technology), rat anti-galectin-3 antibody (American Qualex Inc, San Clemente, CA, USA) or mouse anti-GnT-V antibody 24D11 (provided from Fujirebio, Hachioji, Japan) at 1:500 dilution overnight at 4°C, or with mouse monoclonal anti-β-actin (Sigma-Aldrich, St. Louis, MO, USA) at 1:5000 for 30 min at room temperature. The membranes were then washed three times in TBS-T (5 min each wash). Finally, the membranes were incubated with horseradish peroxidase (HRP)-conjugated anti-rabbit, anti-mouse or anti-rat antibodies (1:10 000 dilution) for 60 min at room temperature. Protein bands were detected by chemiluminescence, using the ECL Plus kit (GE Healthcare, Buckinghamshire, UK).

siRNA transfection

Normal human epidermal keratinocytes (1×10^5 cells/ml) were seeded on type-1 collagen-coated plates 1 day prior to transfection. Cells were transfected with siGnT-V or control siRNAs (Invitrogen) at 2 nM using RNAi MAX (Invitrogen), and the culture medium was replaced 48 h later. Cells were used for experiments 48 h after transfection.

MTS cell viability assay

Cellular viability was assessed using CellTiter96® Aqueous One Solution Cell Proliferation Assay (Promega, Madison, WI, USA). Briefly, NHEKs were seeded onto 96-well plates (5000 cells/well

in 100 μl medium). The cells were allowed to attach for 24 h and then transfected with GnT-V or control siRNAs at 2nM using RNAi MAX (Invitrogen) for 48 h. The cells were further incubated with or without HB-EGF for 48 h. Next, 20 μl of MTS reagent was added, and the cells were incubated for 2 h. Optical density was measured at 490 nm with a Micro Plate Reader (Bio-Rad). In mouse study, keratinocytes were isolated from mouse tail skin and were seeded onto 96-well plates (5000 cells/well in 100 μl medium). Cellular viability was assessed on indicated days.

RNA isolation and quantitative real-time polymerase chain reaction

Total RNA was isolated from cells using the SV Total RNA Isolation System (Promega). The product was reverse-transcribed into first-strand complementary DNA (cDNA). Thereafter, the expression of GnT-V was measured using the Power SYBR Green PCR Master Mix (Applied Biosystems, Foster City, CA, USA) according to the manufacturer's protocol. Glyceraldehyde-3-phosphate dehydrogenase (GAPDH) was used to normalize the mRNA. Sequence-specific primers were designed as follows: GnT-V, sense: 5′-ggcagaaaagcagaaccttg, antisense: 5′-gccagatcggtttcctacaa and GAPDH, sense: 5′- ggagtcaacggatttggtcgta-3′, antisense: 5′- gcaacaatatccactttaccagagttaa-3′. Real-time PCR (40 cycles of denaturation at 92°C for 15 s and annealing at 60°C for 60 s) was run on an ABI 7000 Prism (Applied Biosystems).

TPA treatment

Phorbol ester 12-O-tetradecanoyl phorbol-13-acetate (TPA, 25 μM in 200 μl ethanol) or 200 μl ethanol was applied to shaved back skin of 20-week-old WT mice and *Mgat5*$^{-/-}$ mice (n = 5 in each group) three times a week for 4 weeks. The back skin was removed 1 day after the final application for histological analysis.

Statistical analysis

The data are expressed as mean values ± standard deviation (SD). The unpaired Student's t-test was used to determine the level of significance of differences between the two groups.

Analysis of variance for the groups was performed by means of the Kruskal–Wallis test, followed by the Fisher's PLSD for multiple comparisons to allow pairwise testing for significant differences between groups. Statistical significance was defined as $P < 0.05$.

Results

GnT-V regulates the proliferation of NHEKs and mouse keratinocytes

To determine whether GnT-V is involved in keratinocyte proliferation, we performed an MTS cell proliferation assay using GnT-V knockdown NHEKs. Transfection of NHEKs with GnT-V siRNA decreased GnT-V expression by more than 95% compared with control siRNA (Fig. 1a). At the start of culture (day 0), no difference in cell number was observed between GnT-V knockdown and control siRNA-transfected NHEKs (Fig. 1b). After 48 h of culture (day 2), the number of GnT-V knockdown NHEKs was reduced compared to control NHEKs. Treatment with HB-EGF, a paracrine growth factor that is released from keratinocytes and plays a pivotal role in maintaining skin homoeostasis, stimulates the proliferation of NHEK cells. However, this stimulation was significantly suppressed in GnT-V knockdown cells (Fig. 1b).

To confirm the relationship between GnT-V and the proliferation of keratinocytes, we isolated primary keratinocytes from *Mgat5*$^{-/-}$, GnT-V-deficient mice and assessed their proliferative activity using

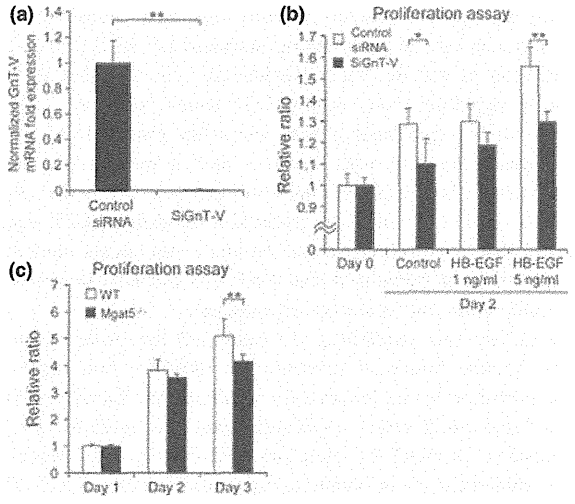

Figure 1. GnT-V functions in NHEK and mouse primary keratinocyte proliferation. (a) GnT-V knockdown in NHEK cells by siRNA transfection (siGnT-V) decreased GnT-V mRNA levels by more than 95%, as assessed by real-time PCR. GAPDH was used as an internal control. (b) NHEKs transfected with siGnT-V were incubated with or without EGF or HB-EGF for 48 h. Cell proliferation was assessed by an MTS assay. (n = 6 per group); *$P < 0.05$, **$P < 0.01$, Fisher's PLSD for control siRNA versus siGnT-V. (c) Proliferation of primary cultured keratinocytes from WT and *Mgat5*$^{-/-}$ mice was assessed by an MTS assay. (n = 6 per group); **$P < 0.01$, Fisher's PLSD for WT versus *Mgat5*$^{-/-}$. Representative results from 1 of 3 independent experiments are shown.

MTS assay. *Mgat5*$^{-/-}$ keratinocytes had significantly reduced proliferative activity compared to WT keratinocytes (Fig. 1c).

Mgat5$^{-/-}$ mouse skin is resistant to TPA-induced epidermal thickening

To further characterize the role of GnT-V in epidermal proliferation *in vivo*, we examined the response of mouse skin to topical application of the phorbol ester 12-O-tetradecanoyl phorbol-13-acetate (TPA), which induces hyperproliferation and inflammation in the skin (16). With vehicle alone treatment, WT and *Mgat5*$^{-/-}$ mice showed similar levels of epidermal thickening, suggesting that GnT-V is not involved in maintaining the normal structure of the epidermis (Fig. 2a, upper panel). Compared to the vehicle control, TPA treatment induced a 1.66 ± 0.23 (mean ± SD) fold increase in epidermal thickness in WT mice and a 1.25 ± 0.25 (mean ± sd) fold increase in epidermal thickness in *Mgat5*$^{-/-}$ mice (Fig. 2a, b). To determine whether the reduced hyperplasia in *Mgat5*$^{-/-}$ mice is a result of a reduction in keratinocyte proliferative activity, we performed Ki-67 immunohistochemistry in TPA-treated mouse skin. The number of Ki-67-positive cells was lower in TPA-treated *Mgat5*$^{-/-}$ epidermis compared with WT epidermis (Fig. 2c, d).

Cell surface EGFR expression is decreased in *Mgat5*$^{-/-}$ mouse keratinocytes

Glycosylation of growth factor receptors by GnT-V is reported to enhance signalling by inhibiting the rapid internalization of receptors from the cell surface (8). Because EGFR-mediated signalling plays a crucial role in maintaining skin homoeostasis, we examined the expression and localization of EGFR in WT and *Mgat5*$^{-/-}$ keratinocytes by immunohistochemistry. Cell surface EGFR staining was weaker in cells from *Mgat5*$^{-/-}$ mice than in WT (Fig. 3a). Western blots of EGFR and galectin-3 in keratinocytes from WT and *Mgat5*$^{-/-}$ *mice* revealed that the expression levels of EGFR and

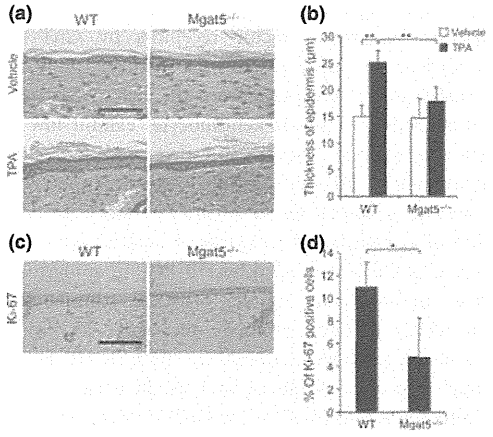

Figure 2. *Mgat5*$^{-/-}$ mouse keratinocytes are resistant to TPA-induced proliferation (a) Haematoxylin and eosin staining of ethanol-treated and TPA-treated mouse skin. (n = 5 per group); Scale bar = 100 μm (b) Epidermal thickness of ethanol-treated and TPA-treated mouse skin. Intrafollicular epidermal thickness was calculated by averaging the thickness of five regions in each section. Three sections from each mouse were evaluated. Bars show the mean epidermal thickness ± SD of each group. (c) Ki-67 immunohistochemistry in TPA-treated skin. (n = 6 per group); Scale bar = 100 μm. (d) The percentage of nuclear Ki-67-positive cells out of the total number of cells was calculated. Three sections from each mouse were evaluated. Bars show the mean ± SD of each group. *P < 0.05, **P < 0.01, Student's t-test.

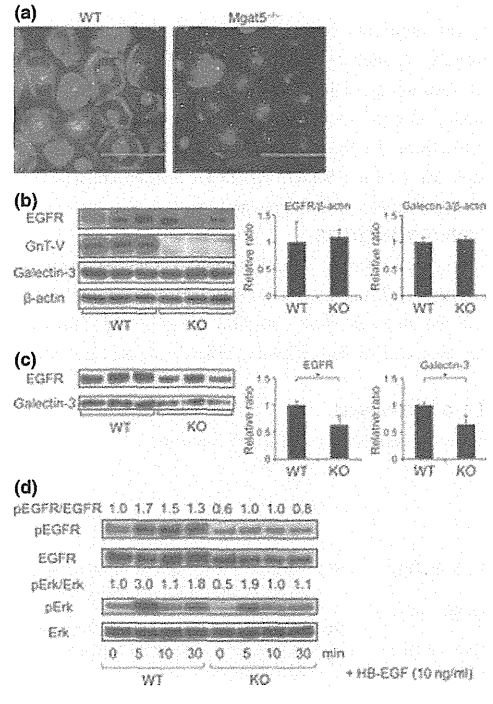

Figure 3. EGFR cell surface expression and EGFR signalling are decreased in *Mgat5*$^{-/-}$ mouse keratinocytes. (a) Representative EGFR (green) and Hoechst 33342 (blue) staining of keratinocytes from WT and *Mgat5*$^{-/-}$ mice. (n = 3 per group); Scale bar = 50 μm (b) EGFR and galectin-3 Western blotting of whole cell extracts from WT and *Mgat5*$^{-/-}$ mouse keratinocytes. Bars show the results of densitometric analysis relative to β-actin. Mean ± SD of each group is shown. (c) EGFR and galectin-3 Western blotting of membrane fractions from WT and *Mgat5*$^{-/-}$ mouse keratinocytes. Bars show the results of densitometric analysis. Mean ± SD of each group is shown. *P < 0.05, Student's t-test. (d) EGFR and Erk phosphorylation of WT and *Mgat5*$^{-/-}$ mouse keratinocytes was evaluated at the indicated time points (0, 5, 10 and 30 min) after stimulation with HB-EGF (10 ng/ml). The numbers indicate densitometric analysis of pEGFR relative to total EGFR and pErk relative to total Erk. Representative results from 1 of 2 independent experiments are shown.

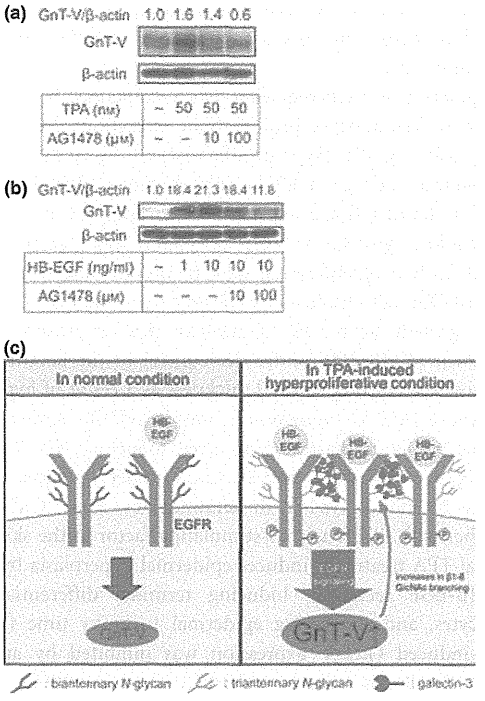

Figure 4. TPA and HB-EGF increase GnT-V expression in NHEKs. (a) Western blotting for detecting GnT-V at 24 h after adding 50 nM TPA with or without EGFR inhibitor AG1478 to the conditioned media of NHEKs. AG1478 was added to the conditioned media 1 h before TPA treatment. Representative results from 1 of 3 independent experiments are shown. (b) GnT-V Western blotting of NHEKs treated with HB-EGF at the indicated doses for 24 h with or without the EGFR inhibitor AG1478. AG1478 was added to the conditioned media 1 h before HB-EGF treatment. Representative results from 1 of 3 independent experiments are shown. (c) Model for GnT-V function in TPA-induced hyperproliferative condition.

galectin-3 were decreased in a cellular membrane fraction but not in a whole cell lysates of *Mgat5*$^{-/-}$ mouse keratinocytes (Fig. 3b, c). To determine whether this decrease in EGFR expression results in downregulation of EGFR signalling, we measured the level of EGFR and Erk phosphorylation induced by HB-EGF (10 ng/ml). As expected, both EGFR and Erk phosphorylations were decreased after HB-EGF treatment in *Mgat5*$^{-/-}$ mouse keratinocytes (Fig. 3d).

Treatment with TPA and HB-EGF increases expression of GnT-V

To further investigate the role of GnT-V in epidermal thickening induced by TPA treatment, we performed Western blots for GnT-V using NHEKs treated with HB-EGF and TPA. GnT-V expression was dramatically increased with TPA treatment (Fig. 4a). TPA is also known to stimulate the secretion of HB-EGF, a major growth factor for epidermal keratinocytes (17). We found that HB-EGF also increased GnT-V expression in keratinocytes (Fig. 4b). This increase was suppressed by an EGFR inhibitor, AG1478, in a dose-dependent manner, indicating that HB-EGF induces GnT-V expression via EGFR signalling (Fig. 4b). TPA-induced GnT-V expression was also suppressed by adding AG1478 in a dose-dependent manner (Fig. 4a), suggesting that TPA enhances the expression of GnT-V in NHEKs in part through EGFR signalling.

Discussion

In this study, we showed that GnT-V is involved in the proliferation of both human and mouse keratinocytes. Our analysis of *Mgat5*$^{-/-}$ mice indicated that GnT-V regulates keratinocyte prolif-

eration only when the epidermis is exposed to hyperproliferative stimuli, but does not affect keratinocyte proliferation under normal conditions.

The epidermis is a self-renewing tissue maintained by the precise regulation of keratinocyte proliferation, migration, differentiation and apoptosis (18, 19). Hyperproliferation of the epidermis occurs during wound healing, in UV-irradiated skin and in barrier-disrupted skin. During tissue regeneration, a variety of inducible factors, including growth factors, cytokines and hormones, are produced. In hyperproliferating skin, membrane-anchored precursors of HB-EGF are cleaved and released from the cells to act as a paracrine growth factor (20). Transgenic mice overexpressing the soluble form of HB-EGF under the control of the keratin 5 promoter show increased epidermal thickness as a result of hyperplasia (21). Because GnT-V expression is low in NHEKs under normal conditions but is dramatically increased following HB-EGF treatment (Fig. 4b), HB-EGF may function under hyperproliferative conditions to induce GnT-V in keratinocytes. Thus, GnT-V may act together with EGFR as a co-stimulating factor in the skin.

Topical TPA treatment induces epidermal hyperplasia by stimulating HB-EGF secretion, inducing terminal differentiation of keratinocytes, and shortening epidermal turnover time (16, 17). As TPA-induced GnT-V expression was inhibited by an EGFR inhibitor (Fig. 4a), secretion of HB-EGF following TPA treatment plays a role in inducing GnT-V in NHEKs. Besides stimulating HB-EGF secretion, TPA also promotes a strong inflammatory reaction associated with mitogen-activated protein kinases, including AKT, NF-κB, STAT3 and AP-1 (22). Thus, it is possible that GnT-V is induced through such a cell signalling pathway, but further investigation is required to elucidate the mechanism of TPA-induced GnT-V expression.

Among the 300 glycosyltransferases encoded in the genome, GnT-V is one of the most important ones associated with tumor growth and tumor metastasis (23). Several reports indicate a role of GnT-V in growth of cancer cells (5, 24–26), but only a few describe GnT-V function in the proliferation of normal tissues. For instance, GnT-V expression is not detected in normal rat liver, but increases after partial hepatectomy (7). This finding is similar to our results showing that GnT-V expression is increased by epidermal hyperproliferative stimuli. Thus, overexpression of GnT-V appears to be required for cell proliferation, and prolonged enhancement of GnT-V expression might be a factor in the initiation of cancer.

Glycosylation of growth factor receptors by GnT-V allows galectin-3 binding to polylactosamine structures, preventing the rapid internalization of receptors from the cell surface (8). Here, we show that *Mgat5*$^{-/-}$ mouse keratinocytes exhibit low cell surface EGFR and galectin-3 levels and decreased EGFR and Erk phosphorylation after HB-EGF stimuli (Fig. 3). These results suggest that altered glycosylation in *Mgat5*$^{-/-}$ mice also modulates the function of growth factor receptors in keratinocytes. We summarized a role of GnT-V induced by HB-EGF in epidermal hyperproliferative conditions in Fig. 4c. HB-EGF stimulates GnT-V expression, which in turn prolongs the active EGFR half-life, implying a strong positive feedback function in HB-EGF signalling, although a positive feedback that would require a sustained HB-EGF initiating signal to allow for GnT-V upregulation.

In conclusion, we found that GnT-V is important in epidermal hyperproliferation induced by TPA. Shedding of membrane-anchored HB-EGF is induced by various epidermal hyperproliferative stimuli. Soluble HB-EGF induces the expression of GnT-V, which is involved in the synthesis of β1,6 GlcNAc branches. This results in increased polylactosamine structure on growth factor receptors such as EGFR. An increase in galectin-3 binding to the polylactosamine structures of EGFR inhibits EGFR endocytosis, resulting in prolonged and enhanced EGFR signalling.

Acknowledgements

This study was supported by a grant from the Global COE program of Osaka University, funded by the Ministry of Education, Culture, Sports, Science and Technology of Japan and by a Grant-in-Aid for Young Scientists (B), and a Grant-in-Aid for Scientific Research (A), No. 21249038, No. 22791069, from the Japan Society for the Promotion of Science. The authors thank Mr. Kenju Nishida, Ms. Eriko Nobuyoshi, Ms. Sayaka Matsumura and Ms. Yumiko Fujii for research assistance.

Author contributions

Akihiro Kimura, Mika Terao, Arisa Kato and Takaaki Hanafusa performed the research, Akihiro Kimura, Mika Terao, Ichiro Katayama and Eiji Miyoshi designed the research study, Akihiro Kimura and Hiroyuki Murota analysed the data, and Akihiro Kimura, Mika Terao and Eiji Miyoshi wrote the paper.

Conflicts of interest

The authors have declared no conflicting interests.

References

1 Rademacher T W, Parekh R B, Dwek R A. Annu Rev Biochem 1988: **57**: 785–838.
2 Dennis J W, Granovsky M, Warren C E. Biochim Biophys Acta 1999: **1473**: 21–34.
3 Tian H, Miyoshi E, Kawaguchi N *et al.* Pathobiology 2008: **75**: 288–294.
4 Murata K, Miyoshi E, Kameyama M *et al.* Clin Cancer Res 2000: **6**: 1772–1777.
5 Granovsky M, Fata J, Pawling J, Muller W J, Khokha R, Dennis J W. Nat Med 2000: **6**: 306–312.
6 Terao M, Ishikawa A, Nakahara S *et al.* J Biol Chem 2011: **286**: 28303–28311.
7 Miyoshi E, Ihara Y, Nishikawa A *et al.* Hepatology 1995: **22**: 1847–1855.
8 Lajoie P, Partridge E A, Guay G *et al.* J Cell Biol 2007: **179**: 341–356.
9 Partridge E A, Le Roy C, Di Guglielmo G M *et al.* Science 2004: **306**: 120–124.
10 Zhao Y, Sato Y, Isaji T *et al.* FEBS J 2008: **275**: 1939–1948.
11 Gu J, Zhao Y, Isaji T *et al.* Glycobiology 2004: **14**: 177–186.
12 Pastore S, Mascia F, Mariani V, Girolomoni G. J Invest Dermatol 2008: **128**: 1365–1374.
13 Schneider M R, Werner S, Paus R, Wolf E. Am J Pathol 2008: **173**: 14–24.
14 Yoshida A, Kanno H, Watabe D, Akasaka T, Sawai T. Arch Dermatol Res 2008: **300**: 37–45.
15 Terao M, Murota H, Kitaba S, Katayama I. Exp Dermatol 2010: **19**: 38–43.
16 Parkinson E K. Br J Cancer 1985: **52**: 479–493.
17 Izumi Y, Hirata M, Hasuwa H *et al.* EMBO J 1998: **17**: 7260–7272.
18 Mihaly J, Gamlieli A, Worm M, Ruhl R. Exp Dermatol 2011: **20**: 326–330.
19 Panzella L, Wakamatsu K, Monfrecola G, Ito S, Ayala F, Napolitano A. Exp Dermatol 2011: **20**: 288–290.
20 Higashiyama S, Iwabuki H, Morimoto C, Hieda M, Inoue H, Matsushita N. Cancer Sci 2008: **99**: 214–220.
21 Shirakata Y. J Dermatol Sci 2010: **59**: 73–80.
22 Contreras-Jurado C, Garcia-Serrano L, Gomez-Ferreria M, Costa C, Paramio J M, Aranda A. J Biol Chem 2011: **286**: 24079–24088.
23 Demetriou M, Nabi I R, Coppolino M, Dedhar S, Dennis J W. J Cell Biol 1995: **130**: 383–392.
24 Li D, Li Y, Wu X *et al.* J Immunol 2008: **180**: 3158–3165.
25 Cheung P, Dennis J W. Glycobiology 2007: **17**: 767–773.
26 Zhou X, Chen H, Wang Q, Zhang L, Zhao J. Clin Invest Med 2011: **34**: E155–162.

Published OnlineFirst on April 6, 2012; DOI:10.1158/1055-9965.EPI-11-1183

Cancer Epidemiology, Biomarkers & Prevention

Research Article

Increased Levels of Tetra-antennary *N*-Linked Glycan but Not Core Fucosylation Are Associated with Hepatocellular Carcinoma Tissue

Anand Mehta[1], Pamela Norton[1], Hongyan Liang[1], Mary Ann Comunale[1], Mengjun Wang[1], Lucy Rodemich-Betesh[1], Alex Koszycki[1], Katsuhisa Noda[2], Eiji Miyoshi[3], and Timothy Block[1]

Abstract

Background: Alterations in glycosylation have long been associated with the development of cancer. In the case of primary hepatocellular carcinoma (HCC), one alteration that has often been associated is increased amounts of fucose attached to the *N*-glycans of serum proteins secreted by the liver.

Methods: In an effort to determine the origin of this increased fucosylation, we have conducted *N*-linked glycan analysis of HCC tissue, the surrounding nontumor tissue, and compared this to tissue from a nondiseased adult liver.

Results: Surprisingly, no difference in the level of fucosylation was observed from the three donor groups, suggesting that the increased levels of fucosylation observed in serum of those with HCC is not the result of increased synthesis of fucosylated proteins in the cancer tissue. On the other hand, increased levels of a tetra-antennary glycan were observed in the HCC tissue as compared with the surrounding tissue or to the nondiseased livers.

Conclusions: This represents, to our knowledge, one of the first reports associating increased levels of branching with the development of HCC.

Impact: The identification of increased levels of tetra-antennary glycan on liver tumor tissue, as opposed to adjacent or nondiseased tissue may lead to improved detection of HCC. *Cancer Epidemiol Biomarkers Prev; 1–9.* ©*2012 AACR.*

Introduction

Infection with hepatitis B virus (HBV) or hepatitis C virus (HCV) is the major etiology of hepatocellular carcinoma (HCC; refs. 1–4). Both HBV and HCV cause acute and chronic liver infections, and most chronically infected individuals remain asymptomatic for many years (5). Between 10% and 40% of all chronic HBV carriers eventually develop primary liver cancer (HCC), and it is estimated that more than one million people worldwide die of HBV/HCV-associated liver cancer (2, 6, 7). Indeed, HBV and HCV infections are associated with more than 80% of all HCC cases worldwide and can be as high as 96% in regions where these viruses are endemic (3).

The progression from liver disease to liver cancer is often monitored with serum levels of oncofetal glycoprotein, α-fetoprotein (AFP), or the core fucosylated glycoform of AFP (AFP-L3; refs. 8–10). However, AFP can be produced under circumstances other than HCC, including association with other liver diseases (8–10), and it is not elevated in all patients with HCC (11). Therefore, the reliability of AFP levels as a screening tool for HCC has been questioned (12), and more sensitive serum biomarkers for HCC are desired.

Using various proteomic methods to look for biomarkers useful in the early detection of HCC, we identified changes in the levels of *N*-glycan in total serum and in serum depleted of IgG and/or major acute-phase proteins (13–15). The change in glycosylation observed in the serum associated with HCC was an increase in the level of fucosylation, which has also been reported by others. In this study, we expanded our search by analyzing the glycosylation of HCC tissue as compared with the noncancerous adjacent tissue. In addition, we have examined the *N*-linked glycosylation of normal healthy livers. Surprisingly, increased levels of fucosylation were not observed in the HCC tissue as compared with either surrounding tissue or "healthy" tissue. Thus, the increased

Authors' Affiliation: [1]Department of Microbiology and Immunology, Drexel Institute for Biotechnology and Virus Research, Drexel University College of Medicine, Doylestown, Pennsylvania; [2]Department of Gastroenterology, Osaka Rosai Hospital, Nakasonecho, Kitaku, Sakai; and [3]Department of Molecular Biochemistry and Clinical Investigation, Osaka University Graduate School of Medicine, Yamada-oka, Suita, Japan

Note: Supplementary data for this article are available at Cancer Epidemiology, Biomarkers & Prevention Online (http://cebp.aacrjournals.org/).

Corresponding Author: Anand Mehta, Department of Microbiology and Immunology, Drexel Institute for Biotechnology and Virology, Drexel University College of Medicine, 3805 Old Easton Road, Doylestown, PA 18902. Phone: 215-489-4905; Fax: 215-489-4920; E-mail: anand.mehta@drexelmed.edu

doi: 10.1158/1055-9965.EPI-11-1183

Published OnlineFirst on April 6, 2012; DOI:10.1158/1055-9965.EPI-11-1183

Table 1. Patient information

Patient no.[a]	Age/gender[b]	Etiology[c]	T-BIL[d]	AST[e]	ALT[f]	GGTP[g]	AFP[h]
1	69/M	HCV	1.2	142	286	60	12
2	63/M	HCV	0.7	77	73	47	143
3	69/F	HCV	0.8	64	57	103	53/103
4	59/M	HCV	0.5	83	101	121	24
5	59/M	HCV	0.8	102	115	235	12
6	66/M	HCV	0.8	99	206	106	40
7	63/M	HBV	1.4	58	53	180	17
8	65/F	HCV	0.9	35	37	77	13
9	63/F	HBV	0.9	57	47	40	6
10	63/M	HCV	0.5	48	54	53	15
11	53/M	HCV	0.7	157	154	179	96
12	64/M	HCV	0.9	133	141	57	96
13	64/M	NBNC	0.4	48	69	171	12
14	66/F	HBV	1.3	19	14	14	1,276
15	50/F	HBV	NA	38	51	NA	18,500
16	NA	NA	NA	NA	NA	NA	NA

Abbreviation: NBNC, non-HBV and non-HCV liver disease.

[a]Patient pairs. For each patient, HCC and adjacent tissue was obtained.

[b]The gender, male (M) or female (F), and age of the patient.

[c]The etiology of the cancer.

[d]Total bilirubin levels in mg/dL.

[e]Aspartate transaminase in IU/L.

[f]Alanine transaminase in IU/L.

[g]Gamma-glutamyl transpeptidase in IU/L.

[h]AFP in ng/mL.

levels of fucosylation that are observed in sera of patients with HCC, but not in those of benign liver diseases, suggests an abnormal secretion of fucosylated proteins in HCC. In contrast, increased levels of tetra-antennary glycan were observed in the HCC tissue as compared with both the surrounding tissue and the tissue from a normal liver. Tetra-antennary glycans result from increased activity of the *N*-acetylglucosaminyltransferase V (GnT-V) enzyme, which has long been associated with cancer development and metastatic potential (16–19). This is the first report of increased levels of tetra-antennary glycan in HCC tissue. Importantly, this change was found in both AFP-positive and more importantly, AFP-negative tumors, indicating its potential role as a cancer biomarker.

Materials and Methods

Patients

The present study enrolled 16 patients of ages 62.4 ± 4.2 (10 males, 5 females, and 1 NA) with HCC who had undergone surgical resection between January 1992 and December 1997 at Osaka Rosai Hospital (Nakasonecho, Kitaku, Sakai, Japan). For all patients, hepatitis B surface antigen (HBsAg), hepatitis B surface antibody (HBsAb), and HCV antibody were routinely examined by commercially available methods. Positivity for HCV-RNA was confirmed in a subset of patients with HCV. Of the 16 patients enrolled, HBsAg and HCV antibody were positive in 4 and 10 patients, respectively. One patient was double negative for HBV and HCV and another patient had no clinical information. Clinical data of each patients are described in Table 1. All patients with HCC had no history of treatment for HCC before the operation in which liver samples were collected. Tumor samples and nontumor portions of the liver were obtained during the surgical resection and were snap-frozen in liquid nitrogen and stored at −80°C until used. Nontumor tissues were collected at a distance of at least 5 cm from the cancer lesions. All of the liver samples were histologically examined by an experienced pathologist who had no knowledge of the analytic results. This project was approved by the Ethics Committees of Osaka Rosai Hospital hospitals and written informed consent was obtained from patients in this study.

Tissue preparation

Tissue was sliced into fine pieces and dounce homogenized in a 30 mmol/L Tris-HCl pH 7.4 buffer containing 0.3% SDS, 3% dithiothreitol (DTT), 4 mmol/L $MgCl_2$, and a Protease Inhibitor Cocktail (Roche) and placed on ice for 1 hour. The lysate was spun down at 14,000 rpm for 30 minutes and buffer exchanged into PBS at pH 7.2. Protein concentration was assayed using a NanoDrop (ThermoFisher).

Published OnlineFirst on April 6, 2012; DOI:10.1158/1055-9965.EPI-11-1183

Glycan analysis

Four hundred micrograms of protein lysate or 5 μl of human serum was absorbed into a 3 mm dehydrated gel plugs. The protein gel plugs were then reduced by boiling in 35 mmol/L DTT for 5 minutes, and alkylated at room temperature in 100 mmol/L iodoacetamide. The gel plugs were fixed, 3 × 30 minutes in a solution of 40% methanol and 7% acetic acid. A washing step is conducted by dehydration in acetonitrile, rehydration in 20 mmol/L ammonium bicarbonate, and dehydration with acetonitrile, then dried in a speedVac. Ten microunits of peptide:*N*-glycosidase F (Prozyme) was diluted with 7 μL of 20 mmol/L ammonium bicarbonate, pH 7, and allowed to adsorb into the gel plug. The gel plug was then covered with buffer and allowed to incubate overnight at 37°C. The glycans were eluted from the gel plug by sonication in Milli-Q water 3 times; the pooled elutant was dried down and labeled with a 2-aminobenzamide dye (Ludger) according to the manufacturer's instructions. Excess dye was removed with paper chromatography and the glycans were passed through a 0.22-μm syringe filter. Fluorescently labeled glycans were subsequently analyzed by high-performance liquid chromatography (HPLC) using a TSK-Gel Amide 80 column (Tosoh). The mobile phase consisted of solvent A (50 mmol/L ammonium formate, pH 4.4) and solvent B (acetonitrile). The gradient used was as follows: linear gradient from 20% to 58% solvent A at 0.4 mL/min for 152 minutes followed by a linear gradient from 58% to 100% solvent A for the next 3 minutes. The flow rate was increased to 1.0 mL/min, and the column was washed in 100% solvent A for 5 minutes. Following the washing step, the column was equilibrated in 20% solvent A for 22 minutes in preparation for the next sample run. HPLC analysis was conducted with the Waters Alliance HPLC System, complemented with a Waters fluorescence detector, and quantified with the Millennium Chromatography Manager (Waters Corporation). Glycan structures were identified by calculating the glucose unit value and exoglycosidase digestion, as previously described (20).

Statistical analysis

Descriptive statistics for patients were compared by scatter plots that included the outliers. All values were reported as mean values ± SD unless otherwise stated. Because the data did not follow a typical Gaussian distribution, a nonparametric test (2-tailed, 95% confidence interval, Mann–Whitney *U* test) was used to determine statistical differences between groups. To determine the optimal cutoff value for each marker, the receiver operating characteristic (ROC) curves were constructed using all possible cutoff values for each assay. The area under the ROC (AUROC) curves were constructed and compared as described previously. A 2-tailed *P* value of 0.05 was used to determine statistical significance. All descriptive analyses were conducted using a GraphPad Prism. For combinatorial analysis, AFP values were log transformed to bring the values of all markers into a similar scale, and a centering and scaling approach was taken to normalize data before analysis using a multivariate logistic regression method, using the R package, version 2.8.1.

Results

Fucosylation is not increased in HCC tissue as compared with adjacent or control tissue

In previous work, we and others, have observed increased levels of core fucosylated glycan in the serum of patients with HCC (13–15, 21–25). In an effort to determine whether the cancerous tissue is the source of the increased level of serum core fucosylation we have conducted *N*-linked glycan analysis of normal, tumor, and adjacent nontumor (fibrotic) tissue. Sixteen tumor samples, along with adjacent tissue obtained from patients undergoing tumor resection are described in Table 1. In addition, "normal, healthy" tissue was obtained from 3 independent "control livers" from commercial sources. For all tissue, total protein lysates were made and the amount of total protein was quantified before the *N*-linked glycans attached to total protein were removed enzymatically using peptide:*N*-glycosidase F and labeled with a fluorescent dye before analysis of the *N*-linked glycans via sequential exoglycosidase digestion (26–28).

Figure 1A and B shows the simplified desialylated glycoprofile for a representative patient set (HCC and surrounding tissue) following treatment with neuraminidase (*Arthrobacter ureafaciens*). Each peak corresponds to a different glycan structure (or multiple structures) and as this figure shows, little difference is observed between the adjacent and HCC tissue from the individual patient shown. Sequential exoglycosidase digestion (data not shown) was used to identify the core fucosylated *N*-linked glycan. Two major types of core (α-1,6 linked) fucosylated glycan were observed in the liver tissue, a core fucosylated biantennary glycan and a core fucosylated triantennary glycan. The levels of each of these structures in the adjacent and HCC tissue are shown in Fig. 1C and D. As this figure shows, the level of core fucosylation is not substantially increased in the patients with HCC as compared with the adjacent tissue or normal tissue from a donor liver. Figure 1C shows the relative levels of the core fucosylated biantennary glycan in all 16 tissue pairs. As summarized in Table 2, the core fucosylated biantennary peak had a mean value of 13.34% of the total glycan pool in the adjacent tissue, and 14.81% in the HCC tissue. This compares with an average of 11.6% in the control tissue (Table 3). None of these differences were statistically different. Pairwise statistical analysis was also used to determine whether difference in core fucosylation could be observed between patient pairs; however, no statistically significant differences could be observed.

As Fig. 1A and B highlight, a core fucosylated triantennary glycan was also observed (peak 5). The levels of this glycan in the 16 tissue pairs is shown in Fig. 1D and similar to the results observed in Fig. 1C, the levels of this core fucosylated species are not consistently altered in the

Published OnlineFirst on April 6, 2012; DOI:10.1158/1055-9965.EPI-11-1183

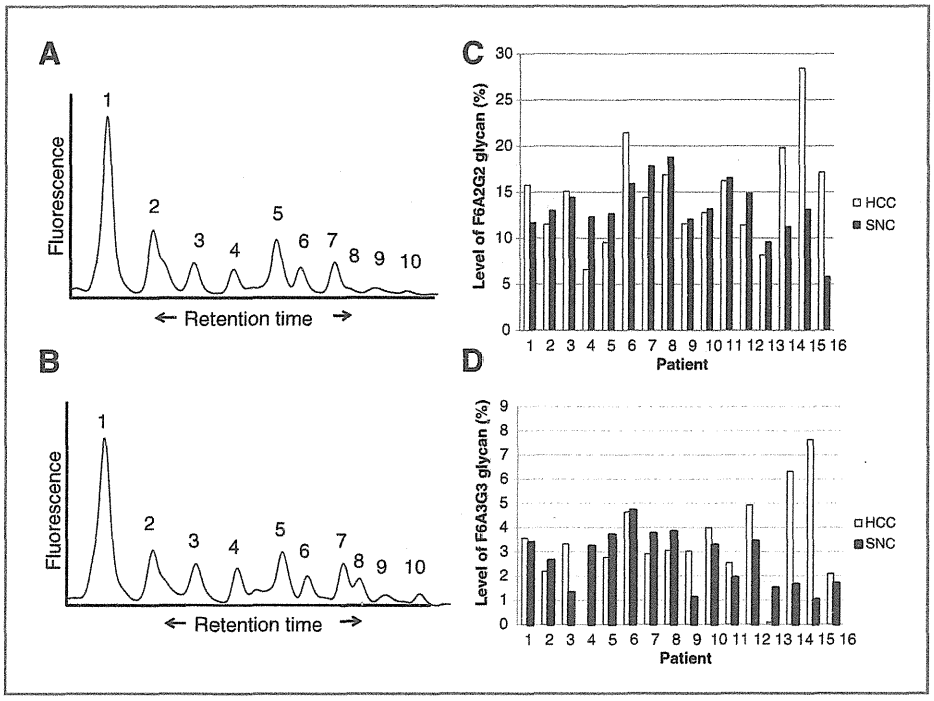

Figure 1. *N*-Linked glycosylation of total protein from representative HCC tissue and adjacent liver tissue. Desialylated *N*-linked glycan profile of representative adjacent liver tissue (A) or HCC tissue (B) from one matched pair. Identified species are indicated as follows, using terminology described elsewhere (45): peak 1, A2G2; peak 2, F(6)A2G2; peak 3, M7; peak 4, A3G3; peak 5, comigrating M8 and F(6)A3G3; peak 7, M9; peak 8, A4G4; peak 9, F(6)A4G4. Peaks 6 and 10 are incompletely characterized, although peak 6 contains one or more structures containing outer arm fucose. C, the level of the F(6)A2G2 glycan in the matched pairs of tissue. The percentage of the F(6)A2G2 glycan as a function of the total glycan profile is shown. D, the level of the F(6)A3G3 glycan in the matched pairs of tissue. As with (C), the percentage of the F(6)A3G3 glycan is a function of the total glycan profile. For Figures C and D, HCC, hepatocellular carcinoma tissue; SNC, surrounding non cancer tissue.

HCC tissue as compared with the adjacent tissue. As summarized in Table 2, the core fucosylated triantennary peak had a mean value of 2.66% of the total glycan pool in the adjacent tissue, and 3.32% in the HCC tissue. This compares with an average of 2.9% in the control tissue (Table 3). These numbers were not statistically different ($P > 0.05$).

Increased branching is observed in HCC tissue

In contrast to core fucosylation, which was not consistently altered in the HCC tissue, as compared with the adjacent tissue, increased levels of tetra-antennary glycan (A4G4) were observed in the HCCs when compared with the adjacent tissue. Figure 2 shows a focus of the tetra-antennary *N*-linked glycan following treatment with neuraminidase (*Arthrobacter ureafaciens*) and α-(1-2,3,6)-jack bean mannosidase (Fig. 2A). Subsequently, the peak preliminarily identified as a A4G4 glycan was collected and digested individually with almond meal and bovine kidney fucosidase (for alpha 1-3,4,6-linked fucose; Fig. 2B) and bovine jack bean β-(1-4,6) galactosidase (Fig. 2C). As Fig. 2 shows, whereas treatment with the fucosidases did not alter this peak (Fig. 2B), indicating that this peak is not fucosylated, treatment with the beta-galactosidase shifted the peak to a level consistent with an A4G0 glycan (an agalactosylated tetra-antennary glycan). Digestion of this structure with hexosaminidase (Glyko; β-*N*-Acetyl-hexosaminidase/HEXase I) digested this structure to the

Table 2. Fucosylated and corresponding nonfucosylated glycan structures associated with HCC and adjacent tissue

Glycan[a]	Tumor mean[b] (±SD)	Nontumor mean[c] (±SD)	*P*
A2G2	37.93 (±4.70)	38.25 (1.95)	>0.05
F(6)A2G2	14.81 (±5.44)	13.34 (±3.17)	>0.05
A3G3	7.06 (±2.42)	6.40 (±1.74)	>0.05
F(6)A3G3	3.32 (±1.96)	2.66 (±1.16)	>0.05
A4G4	2.87 (±1.03)	1.55 (±0.65)	0.0003
F(6)A4G4	1.76 (±0.84)	1.49 (±0.65)	>0.05

Abbreviations: A2G2, biantennary glycan; A3G3, triantennary glycan; A4G4, tetra-antennary glycan; F(6)A2G2, core fucosylated biantennary glycan; F(6)A3G3, core fucosylated triantennary glycan; F(6)A4G4, core fucosylated tetra-antennary glycan.

[a]Key glycans identified in HCC and adjacent tissue.

[b]The mean percentage of each glycan in the total glycan profile of the tumor tissue.

[c]The mean percentage of each glycan in the total glycan profile of the adjacent (nontumor) tissue.

Published OnlineFirst on April 6, 2012; DOI:10.1158/1055-9965.EPI-11-1183

Table 3. *N*-linked glycan content of normal liver tissues

No[a]	Glycan[b]	Liver 1[c]	Liver 2[d]	Liver 3[e]	Liver mean[d] (±SD)
1	A2G2	38.05	37.3	29.36	34.9 (±4.8)
2	F(6)A2G2	11.45	10.15	13.19	11.6 (±1.5)
3	M7	7.88	9.61	8.89	8.79 (±0.87)
4	A3G3	5.75	5.91	4.83	5.5 (±.58)
5*	F(6)A3G3	1.95	3.91	2.87	2.9 (±0.98)
5*	M7	7.88	9.61	8.89	8.79 (±0.87)
7	M9	12.39	10.31	12.33	11.68 (±1.2)
8	A4G4	2.13	1.45	1.20	1.59 (±0.48)
9	F(6)A4G4	1.35	0.41	2.13	1.3 (±0.86)

Abbreviations: A2G2, biantennary glycan; A3G3, triantennary glycan; A4G4, tetra-antennary glycan; F(6)A2G2, core fucosylated biantennary glycan; F(6)A3G3, core fucosylated triantennary glycan; F(6)A4G4, core fucosylated tetra-antennary glycan; M7, Mannose 7 glycan; M8, Mannose 8 glycan; M9, Mannose 9 glycan.

[a]The glycans as numbered in Fig. 1, asterisks indicate comigrating peaks that were subject to exoglycosidase digestion to quantify.

[b]Key glycans associated with tissue examined.

[c]The mean percentage of each glycan in the total glycan profile of the healthy liver tissue.

[d]The mean level of each glycan.

chitobiose core (M3N2), confirming that this peak consisted of a tetra-antennary *N*-linked glycan. The levels of the tetra-antennary N-linked glycan in the HCC and adjacent tissue are shown in Fig. 2D. As this figure shows, the level of the tetra-antennary glycan was increased in 14 of 16 HCC samples, as compared with the adjacent tissue. The levels of the tetra-antennary glycan in normal tissue were similar to what was observed in the adjacent tissue (see Tables 2 and 3). The complete profile of all 16 tissue pairs, with the A4G4 peak indicated are shown in Supplementary Fig. S1.

The mean level of the A4G4 glycan in the HCC tissue was 2.87% of the total glycan pool and 1.55% in the adjacent tissue. Although this is less than a 2-fold difference, 14 of 16 of the HCC tissues were elevated for the glycan relative to the matched nontumor samples, and the mean difference was statistically different ($P = 0.0003$). The level of this glycan in normal liver was 1.59, very similar to the level observed in the nontumor tissue (Table 3).

In an effort to further confirm the results obtained by *N*-linked glycan sequencing, we conducted a lectin blot of total pooled protein from either the HCC or adjacent

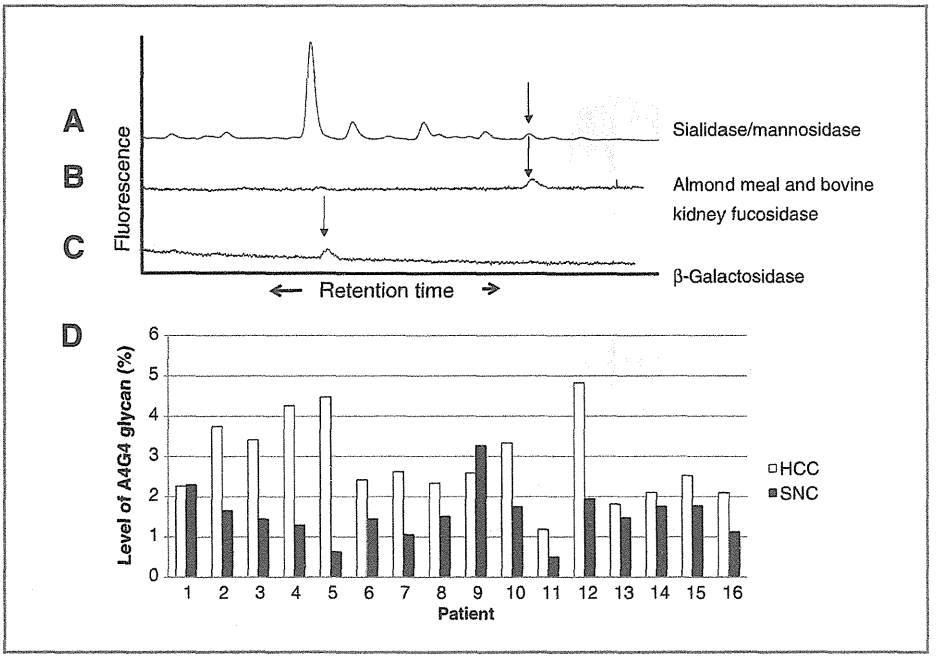

Figure 2. Increased levels of tetra-antennary glycan are associated with HCC tissue. A focus on the tetra-antennary glycan showing (A4G4) the digestion with (A) sialidase (*Arthrobacter ureafaciens*) and jack bean mannosidase, (B) a mixture of bovine kidney (1,6) and almond meal α-(1-3,4) fucosidases, and (C) jack bean β-(1-4,6) galactosidase. The A4G4 peak was collected after treatment with the mannosidase and digested individually. Treatment with jack bean β-(1-4,6) galactosidase results in the removal of the terminal galactose residues and the creation of an A4G0 glycan as indicated by the arrow. D, the level of the A4G4 glycan in the matched pairs of tissue. The percentage of the A4G4 glycan as a function of the total glycan profile is shown. For Figures C and D, HCC, hepatocellular carcinoma tissue; SNC, surrounding non cancer tissue.

Published OnlineFirst on April 6, 2012; DOI:10.1158/1055-9965.EPI-11-1183

tissue. In Fig. 3B, the fucose binding Aleuria aurantia lectin (AAL) was used to determine the level of fucosylation in the HCC and the adjacent tissue. Consistent with the results obtained via *N*-linked glycan sequencing, the AAL lectin blot showed a similar banding pattern in the HCC tissue and in the adjacent tissue, indicating no major change in fucosylation in HCC tissue.

Changes in branching were analyzed using the Datura stramonium lectin (DSL), which has high affinity toward tri- and tetra-antennary complex-type oligosaccharides. As Fig. 3C shows, consistent with the results obtained in Fig. 2, there was substantially more binding of the DSL lectin with the HCC tissue, as compared with the adjacent tissue, suggesting increased levels of branching in the HCC tissue.

Increased tetra-antennary glycan associated with serum glycoproteins in the serum of patient with HCC

In an effort to determine whether the increased level of branched *N*-linked observed in the tissue of patients with HCC could be seen in the serum of patients, we have conducted glycan analysis on serum from 9 HCC and 8 cirrhotic patients. The *N*-linked glycan profile, with a focus on the A4G4 glycan, for 4 representative HCC and 4 cirrhotic, patients is shown. As Fig. 4A shows, there is an increase in the level of the A4G4 glycan in the HCC samples as compared with the cirrhotic samples. Figure 4B shows the level of the A4G4 glycan in all 9 HCC and 8 cirrhotic samples. As this figure shows, the level of A4G4 glycan in the HCC samples ranged from 1.33% of the total glycan pool to 4.8% of the total glycan pool with a media value of 3.00 (±1.13). In the patients with cirrhosis the level of A4G4 glycan ranged from 1.0% of the total glycan pool to 3.0% of the total glycan pool with a median value of 1.98 (±0.653). Although the sample size is small, the difference was statistically significant ($P = 0.032$).

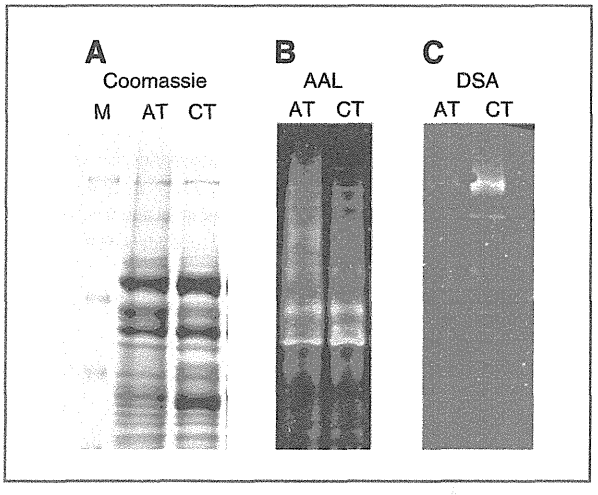

Figure 3. Lectin blotting of HCC and adjacent tissue. Pooled HCC or adjacent tissue was examined by (A) Coomassie staining for total protein, (B) via the AAL for fucosylated proteins, or (C) the DSA for the detection of branched glycan. As this figure shows, consistent with the glycan data, whereas there is no difference in the level of fucosylation in the HCC and adjacent tissue (B) there is a significant difference in the level of branched glycan in the HCC tissue as compared with the adjacent tissue. M, markers; AT, adjacent tissue; and CT, cancer tissue.

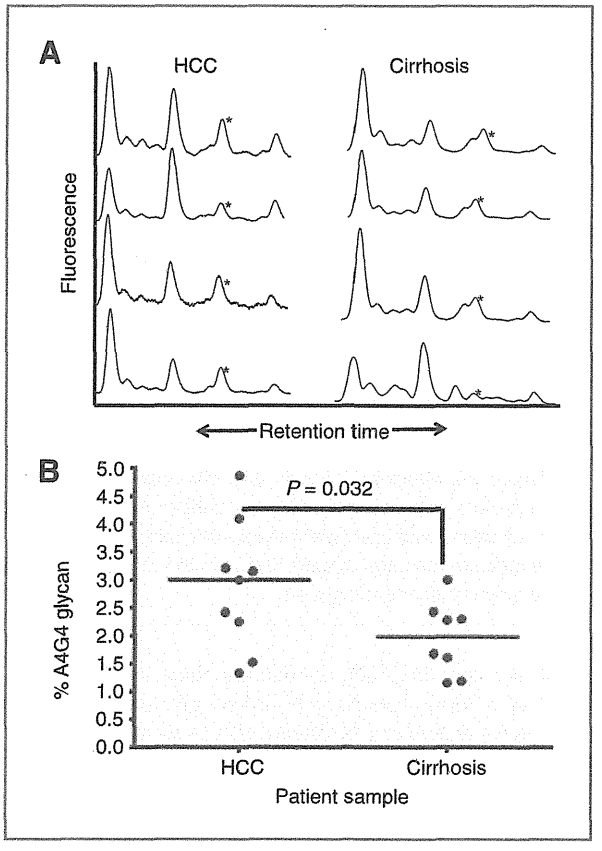

Figure 4. Increased levels of branching on serum glycoproteins from patients with HCC. A, focus on larger branched glycans from 4 representative cirrhotics, and 4 representative HCC samples highlighting specific changes in glycosylation observed in HCC. The A4G4 peak is indicated with an asterisk. As in Fig. 2, sequential exoglycosidase digestion was used to identify *N*-linked glycan. B, scatter plot of the A4G4 glycan from 9 HCC and 8 cirrhotic patients showing the level of the A4G4 glycan in all patients. The solid line indicates the median level and the *P* value is indicated.

Discussion

Changes in *N*-linked glycosylation on serum proteins have been associated by us and by others with liver cancer. The most prominent change has been the increased levels of α-1,6- and α-1,3–linked fucosylation (13–15, 21, 22, 29–35). In an effort to identify the source of this increase we have conducted *N*-linked glycosylation analysis of HCC tissue, surrounding tissue and liver tissue from nondiseased livers. Surprisingly, the normal, HCC, and tumor-adjacent tissue had similar levels of fucosylation, suggesting that the increase in liver-derived fucosylated proteins observed in the circulation is not the result of increased production from either the HCC tissue or the surrounding tissue. Previous reports have indicated that the level of the fucosyltransferases involved in core fucosylation were

Published OnlineFirst on April 6, 2012; DOI:10.1158/1055-9965.EPI-11-1183

similar in cancer and cirrhotic tissue (36). Our glycan analysis is consistent with this finding and extends it by showing that the levels of core fucosylation are similar in both diseased and healthy livers.

One hypothesis is that it is not the production of fucosylated proteins that is greater in HCC but rather increased secretion into the circulation that is responsible for the increased level of fucosylated proteins into the serum (37). The results presented here would support this hypothesis. Indeed, the level of core fucosylated glycan that was observed in liver tissue was much greater than that observed in the circulation of all groups, including individuals with no known liver disease. Interestingly, the level of fucosylation observed in the tissue was similar to what was observed in the serum of patients with HCC (>8.0%), further supporting the hypothesis that altered secretion is the main reason for increased level of fucosylated glycan in the serum of patients with HCC. It is noted that fucosylation changes could be specific to a small set of proteins that are masked by the overall glycan analysis. In a rodent model, only certain glycoproteins were fucosylated in serum, whereas most all glycoproteins were fucosylated in bile (38). Preliminary data suggest that certain kinds of fucosylated proteins were selectively secreted into bile ducts but not into the conditioned medium in HepG2 cells (Nakagawa and colleagues, manuscript in preparation). These possibilities remain to be tested through the glycan analysis of specific proteins following resolution via 2-dimensional electrophoresis.

One change that was observed in HCC tissue was an increase in tetra-antennary *N*-linked glycan. Tetra-antennary *N*-linked glycans arise from the action of the enzyme GnT-V (16), which catalyzes the addition of β-1,6-GlcNAc to the growing *N*-linked glycan to form tri- and tetra-antenna–like oligosaccharides. Increased branching is associated with metastasis and has been associated with alterations in the hexosamine cycle and activation of the AKT pathway (19, 39–42). It has also been reported that expression of GnT-V in the liver was dramatically enhanced in the hepatocarcinogenesis of a rodent model. Increases in β-1,6-GlcNAc structure through upregulation of GnT-V have long been associated with cancers but this report represents the first oligosaccharide analyses with liver cancer tissue. The result was consistent with immunohistochemical analysis of GnT-V in HCC tissue (43) and is consistent with the hypothesis that the elevated expression of UDP-*N*-acetylglucosamine: α-mannoside β-1,6 *N*-acetylglucosaminyltransferase (GnT-V) is an early event in hepatocarcinogenesis.

There are reports in the literature that increased branching of *N*-glycans correlates with reduced intercellular adhesion of epithelial cells (44). These published observations and our findings reported here lead us to propose the following working model (Fig. 5). We speculate that HCC is associated with an increase in tetra-antennary glycan addition to proteins involved cell–cell adhesion and/or tight junction integrity. The resulting weaker cell–cell junctions permit "leaking" of core fucosylated glycoproteins from the biliary system, which are predominantly fucosylated (32), into the blood (and potentially other molecules that are bile specific). This model would account for the apparent discrepancy between core fucose levels present in the serum (and elevated in HCC) versus the tissue (nondifference between tumor and nontumor). Further characterization of the proteins that carry the tetra-antennary glycans will be required to test the model.

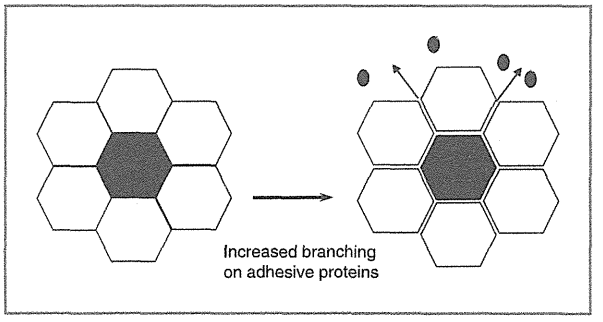

Figure 5. Proposed model. Left, in the normal liver, hepatocytes (white hexagons) surround the biliary space (black hexagons). Tight junctions present near the apical (biliary) surfaces of the hepatocytes isolate bile contents from basolateral contents (blood). Right, as HCC develops, the impermeable barrier weakens, permitting leakage of core fucosylated glycoproteins (black ovals) into the bloodstream.

The identity of the proteins that contain tetra-antennary glycan are unclear but under investigation. It is understood that the level of tetra-antennary glycan was low in the HCC samples and represents only a minor species of the total glycan pool. This is not unexpected as conformationally, not all proteins will have the space to allow for a tetra-antennary glycan. Tetra-antennary glycans are usually observed on cell surface molecules, such as growth factor receptors and adhesion molecules. While these molecules are partially cleaved from the cell surface, it might be difficult to find them in circulation as they would represent only a minor fraction of serum glycoproteins. More advances in glycotechnology for oligosaccharide analysis may be required to fully characterize the *N*-glycan and to identify the proteins containing these alterations.

In conclusion, we have conducted *N*-linked glycan analysis of HCC and adjacent tissue in an effort to determine whether the increase in core fucosylation found on liver-derived serum proteins from patients with HCC was a result of increased fucosylation. Surprisingly, no increase in fucosylation was observed in HCC. In contrast, increased levels of branching, most notably, increased levels of tetra-antennary glycan were observed.

Disclosure of Potential Conflicts of Interest

No potential conflicts of interest were disclosed.

Authors' Contributions

Conception and design: A.S. Mehta, P. Norton, H. Liang, E. Miyoshi, T. Block

Development of methodology: A.S. Mehta, H. Liang, M.A. Comunale, M. Wang

Published OnlineFirst on April 6, 2012; DOI:10.1158/1055-9965.EPI-11-1183

Acquisition of data (provided animals, acquired and managed patients, provided facilities, etc.): P. Norton, H. Liang, M.A. Comunale, M. Wang, A. Koszycki
Analysis and interpretation of data (e.g., statistical analysis, biostatistics, computational analysis): A.S. Mehta, P. Norton, H. Liang, L. Rodemich-Betesh, A. Koszycki, T. Block
Writing, review, and/or revision of the manuscript: A.S. Mehta, P. Norton, H. Liang, M.A. Comunale, M. Wang, T. Block
Administrative, technical, or material support (i.e., reporting or organizing data, constructing databases): A.S. Mehta, H. Liang, L. Rodemich-Betesh, K. Noda, E. Miyoshi, T. Block
Study supervision: A.S. Mehta

Grant Support

This work was supported by grants R01 CA120206 and R01 CA136607 from the National Cancer Institute (NCI), the Hepatitis B Foundation, and an appropriation from The Commonwealth of Pennsylvania.

The costs of publication of this article were defrayed in part by the payment of page charges. This article must therefore be hereby marked *advertisement* in accordance with 18 U.S.C. Section 1734 solely to indicate this fact.

Received December 22, 2011; revised March 9, 2012; accepted March 26, 2012; published OnlineFirst April 6, 2012.

References

1. Di Bisceglie AM. Hepatocellular carcinoma: molecular biology of its growth and relationship to hepatitis B virus infection. Med Clin North Am 1989;73:985–97.
2. Block TM, Mehta AS, Fimmel CJ, Jordan R. Molecular viral oncology of hepatocellular carcinoma. Oncogene 2003;22:5093–107.
3. Marrero JA. Hepatocellular carcinoma. Curr Opin Gastroenterol 2006;22:248–53.
4. Sallie R, Di Bisceglie AM. Viral hepatitis and hepatocellular carcinoma. Gastroenterol Clin North Am 1994;23:567–79.
5. Lok A, McMahon B. Chronic hepatitis B. Hepatology 2001;34: 1225–41.
6. El Serag HB, Mason AC, Key C. Trends in survival of patients with hepatocellular carcinoma between 1977 and 1996 in the United States. Hepatology 2001;33:62–65.
7. Sarbah SA, Gramlich T, Younoszai A, Osmack P, Goormastic M, Grosso L, et al. Risk factors for hepatocellular carcinoma in patients with cirrhosis. Dig Dis Sci 2004;49:850–3.
8. Alpert ME, Uriel J, de Nechaud B. Alpha-1 fetoglobulin in the diagnosis of human hepatoma. N Engl J Med 1968;278:984–6.
9. Ruoslahti E, Salaspuro M, Pihko H, Andersson L, Seppala M. Serum alpha-fetoprotein: diagnostic significance in liver disease. Br Med J 1974;2:527–9.
10. Di Bisceglie AM, Hoofnagle JH. Elevations in serum alpha-fetoprotein levels in patients with chronic hepatitis B. Cancer 1989;64:2117–20.
11. Marrero JA, Romano PR, Nikolaeva O, Steel L, Mehta A, Fimmel CJ, et al. GP73, a resident Golgi glycoprotein, is a novel serum marker for hepatocellular carcinoma. J Hepatol 2005;43:1007–12.
12. Sherman M. Hepatocellular carcinoma: epidemiology, risk factors, and screening.Semin Liver Dis 2005;25:143–54.
13. Comunale MA, Lowman M, Long RE, Krakover J, Philip R, Seeholzer S, et al. Proteomic analysis of serum associated fucosylated glycoproteins in the development of primary hepatocellular carcinoma. J Proteome Res 2006;5:308–15.
14. Comunale MA, Wang M, Hafner J, Krakover J, Rodemich L, Kopenhaver B, et al. Identification and development of fucosylated glycoproteins as biomarkers of primary hepatocellular carcinoma. J Proteome Res 2009;8:595–602.
15. Block TM, Comunale MA, Lowman M, Steel LF, Romano PR, Fimmel C, et al. Use of targeted glycoproteomics to identify serum glycoproteins that correlate with liver cancer in woodchucks and humans. Proc Natl Acad Sci U S A 2005;102:779–84.
16. Srivastava OP, Hindsgaul O, Shoreibah M, Pierce M. Recognition of oligosaccharide substrates by N-acetyl-glucosaminyltransferase-V. Carbohydr Res 1988;179:137–61.
17. Miyoshi E, Nishikawa A, Ihara Y, Gu J, Sugiyama T, Hayashi N, et al. N-acetylglucosaminyltransferase III and V messenger RNA levels in LEC rats during hepatocarcinogenesis. Cancer Res 1993;53:3899–902.
18. Yoshimura M, Nishikawa A, Ihara Y, Taniguchi S, Taniguchi N. Suppression of lung metastasis of B16 mouse melanoma by N-acetylglucosaminyltransferase III gene transfection. Proc Natl Acad Sci U S A 1995;92:8754–8.
19. Guo HB, Johnson H, Randolph M, Nagy T, Blalock R, Pierce M. Specific posttranslational modification regulates early events in mammary carcinoma formation. Proc Natl Acad Sci U S A 2010;107: 21116–21.
20. Guile GR, Rudd PM, Wing DR, Prime SB, Dwek RA. A rapid high-resolution high-performance liquid chromatographic method for separating glycan mixtures and analyzing oligosaccharide profiles. Anal Biochem 1996;240:210–26.
21. Miyoshi E, Noda K, Yamaguchi Y, Inoue S, Ikeda Y, Wang W, et al. The alpha1-6-fucosyltransferase gene and its biological significance. Biochem Biophys Acta 1999;1473:9–20.
22. Noda K, Miyoshi E, Gu J, Gao CX, Nakahara S, Kitada T, et al. Relationship between elevated FX expression and increased production of GDP-L-fucose, a common donor substrate for fucosylation in human hepatocellular carcinoma and hepatoma cell lines. Cancer Res 2003;63:6282–9.
23. Noda K, Miyoshi E, Kitada T, Nakahara S, Gao CX, Honke K, et al. The enzymatic basis for the conversion of nonfucosylated to fucosylated alpha-fetoprotein by acyclic retinoid treatment in human hepatoma cells: activation of alpha1-6 fucosyltransferase. Tumour Biol 2002;23:202–11.
24. Ohno M, Nishikawa A, Koketsu M, Taga H, Endo Y, Hada T, et al. Enzymatic basis of sugar structures of alpha-fetoprotein in hepatoma and hepatoblastoma cell lines: correlation with activities of alpha 1-6 fucosyltransferase and N-acetylglucosaminyltransferases III and V. Int J Cancer 1992;51:315–7.
25. Goldman R, Ressom HW, Varghese RS, Goldman L, Bascug G, Loffredo CA, et al. Detection of hepatocellular carcinoma using glycomic analysis. Clin Cancer Res 2009;15:1808–13.
26. Rudd PM, Dwek RA. Rapid, sensitive sequencing of oligosaccharides from glycoproteins. Curr Opin Biotechnol 1997;8:488–97.
27. Rudd PM, Guile GR, Kuster B, Harvey DJ, Opdenakker G, Dwek RA. Oligosaccharide sequencing technology. Nature 1997;388:205–7.
28. Rudd PM, Mattu TS, Zitzmann N, Mehta A, Colominas C, Hart E, et al. Glycoproteins: rapid sequencing technology for N-linked and GPI anchor glycans. Biotechnol Genet Eng Rev 1999;16:1–21.
29. Comunale MA, Rodemich-Betesh L, Hafner J, Wang M, Norton P, Di Bisceglie AM, et al. Linkage specific fucosylation of alpha-1-antitrypsin in liver cirrhosis and cancer patients: implications for a biomarker of hepatocellular carcinoma. PLoS One 2010;5:e12419.
30. Liu XE, Desmyter L, Gao CF, Laroy W, Dewaele S, Vanhooren V, et al. N-glycomic changes in hepatocellular carcinoma patients with liver cirrhosis induced by hepatitis B virus. Hepatology 2007;46:1426–35.
31. Liu Y, He J, Li C, Benitez R, Fu S, Marrero J, et al. Identification and confirmation of biomarkers using an integrated platform for quantitative analysis of glycoproteins and their glycosylations. J Proteome Res 2010;9:798–805.
32. Miyoshi E, Noda K, Yamaguchi Y, Inoue S, Ikeda Y, Wang W, et al. Altered glycosylation of serum transferrin of patients with hepatocellular carcinoma. J Biol Chem 1999;264:2415–23.
33. Miyoshi E, Moriwaki K, Nakagawa T. Biological function of fucosylation in cancer biology. J Biochem 2008;143:725–9.
34. Miyoshi E, Noda K, Yamaguchi Y, Inoue S, Ikeda Y, Wang W, et al. The alpha1-6-fucosyltransferase gene and its biological significance. Biochim Biophys Acta 1999;1473:9–20.
35. Noda K, Miyoshi E, Uozumi N, Gao CX, Suzuki K, Hayashi N, et al. High expression of alpha-1-6 fucosyltransferase during rat hepatocarcinogenesis. Int J Cancer 1998;75:444–50.
36. Noda K, Miyoshi E, Uozumi N, Yanagidani S, Ikeda Y, Gao C, et al. Gene expression of alpha1-6 fucosyltransferase in human hepatoma

Published OnlineFirst on April 6, 2012; DOI:10.1158/1055-9965.EPI-11-1183

tissues: a possible implication for increased fucosylation of alpha-fetoprotein. Hepatology 1998;28:944–52.
37. Nakagawa T, Uozumi N, Nakano M, Mizuno-Horikawa Y, Okuyama N, Taguchi T, et al. Fucosylation of N-glycans regulates the secretion of hepatic glycoproteins into bile ducts. J Biol Chem 2006;281:29797–806.
38. Nakagawa T, Takeishi S, Kameyama A, Yagi H, Yoshioka T, Moriwaki K, et al. Glycomic analyses of glycoproteins in bile and serum during rat hepatocarcinogenesis. J Proteome Res 2010;9:4888–96.
39. Dennis JW, Laferte S, Waghorne C, Breitman ML, Kerbel RS. Beta 1-6 branching of Asn-linked oligosaccharides is directly associated with metastasis. Science 1987;236:582–5.
40. Dennis JW, Granovsky M, Warren CE. Glycoprotein glycosylation and cancer progression. Biochem Biophys Acta 1999;1473:21–34.
41. Mendelsohn R, Cheung P, Berger L, Partridge E, Lau K, Datti A, et al. Complex N-glycan and metabolic control in tumor cells. Cancer Res 2007;67:9771–80.
42. Lau KS, Partridge EA, Grigorian A, Silvescu CI, Reinhold VN, Demetriou M, et al. Complex N-glycan number and degree of branching cooperate to regulate cell proliferation and differentiation. Cell 2007;129:123–34.
43. Ito Y, Miyoshi E, Sakon M, Takeda T, Noda K, Tsujimoto M, et al. Elevated expression of UDP-N-acetylglucosamine: alphamannoside beta1,6 N-acetylglucosaminyltransferase is an early event in hepatocarcinogenesis. Int J Cancer 2001;91:631–7.
44. Vagin O, Tokhtaeva E, Yakubov I, Shevchenko E, Sachs G. Inverse correlation between the extent of N-glycan branching and intercellular adhesion in epithelia. Contribution of the Na,K-ATPase beta1 subunit. J Biol Chem 2008;283:2192–202.
45. Royle L, Mattu TS, Hart E, Langridge JI, Merry AH, Murphy N, et al. An analytical and structural database provides a strategy for sequencing O-glycans from microgram quantities of glycoproteins. Anal Biochem 2002;304:70–90.

THE JOURNAL OF BIOLOGICAL CHEMISTRY VOL. 287, NO. 41, pp. 33973–33982, October 5, 2012

A Novel Core Fucose-specific Lectin from the Mushroom *Pholiota squarrosa*[S]

Received for publication, April 5, 2012, and in revised form, August 4, 2012 Published, JBC Papers in Press, August 7, 2012, DOI 10.1074/jbc.M111.327692

Yuka Kobayashi[‡1], Hiroaki Tateno[§], Hideo Dohra[¶], Kenta Moriwaki[‖], Eiji Miyoshi[‖], Jun Hirabayashi[§], and Hirokazu Kawagishi[‡‡2]**

*From the [‡]J-Oil Mills, Inc., 11, Kagetoricho, Totsuka-ku, Yokohama, Kanagawa 245-0064, Japan, [§]Research Center for Medical Glycoscience, National Institute of Advanced Industrial Science and Technology, Central 2, 1-1-1 Umezono, Ibaraki 305-8568, Japan, [¶]Institute for Genetic Research and Biotechnology, **Graduate School of Science and Technology, and [‡‡]Department of Applied Biological Chemistry, Faculty of Agriculture, Shizuoka University, 836 Ohya, Suruga-ku, Shizuoka 422-8529, Japan, and the [‖]Department of Molecular Biochemistry and Clinical Investigation, Osaka University Graduate School of Medicine, 1-7, Yamada-oka, Suita, Osaka 565-0871, Japan*

Background: Fuc-α1–6 oligosaccharide has a variety of biological functions.
Results: Purification of a novel Fucα 1–6-specific lectin from the mushroom *Pholiota squarrosa*.
Conclusion: The lectin binds only to core α1–6-fucosylated *N*-glycans and not to the other types of fucosylated oligosaccharides.
Significance: The lectin will be a promising tool for analyzing the biological functions of α1–6 fucosylation.

Fucα1–6 oligosaccharide has a variety of biological functions and serves as a biomarker for hepatocellular carcinoma because of the elevated presence of fucosylated α-fetoprotein (AFP) in this type of cancer. In this study we purified a novel Fucα1–6-specific lectin from the mushroom *Pholiota squarrosa* by ion-exchange chromatography and affinity chromatography on thyroglobulin-agarose. The purified lectin was designated as PhoSL (*P. squarrosa* lectin). SDS-PAGE, MALDI-TOF mass spectrometry, and N-terminal amino acid sequencing indicate that PhoSL has a molecular mass of 4.5 kDa and consists of 40 amino acids (NH_2-APVPVTKLVCDGDTYKCTAYLDFGDGRWVAQWDT-NVFHTG-OH). Isoelectric focusing of the lectin showed bands near pI 4.0. The lectin activity was stable between pH 2.0 and 11.0 and at temperatures ranging from 0 to 100 °C for incubation times of 30 min. When PhoSL was investigated with frontal affinity chromatography using 132 pyridylaminated oligosaccharides, it was found that the lectin binds only to core α1–6-fucosylated *N*-glycans and not to other types of fucosylated oligosaccharides, such as α1–2-, α1–3-, and α1–4-fucosylated glycans. Furthermore, PhoSL bound to α1–6-fucosylated AFP but not to non-fucosylated AFP. In addition, PhoSL was able to demonstrate the differential expression of α1–6 fucosylation between primary and metastatic colon cancer tissues. Thus, PhoSL will be a promising tool for analyzing the biological functions of α1–6 fucosylation and evaluating Fucα1–6 oligosaccharides as cancer biomarkers.

Fucose is a monosaccharide that is found on glycoproteins and glycolipids in vertebrates, invertebrates, plants, and microorganisms. Fucosylation comprises the transfer of a fucose residue to oligosaccharides and glycoproteins and is one of the most important oligosaccharide modifications involved in cancer and inflammation (1). Fucosylation is divided into several types, including α1–2, α1–3, α1–4, and α1–6 fucosylation. Among them, α1–6 fucosylation, which is referred to as core fucosylation, is a cancer biomarker for hepatocellular carcinoma (HCC)[3] because of the elevated presence of α1–6-fucosylated AFP (AFP-L3) in this type of cancer. The α1–6 fucosylation of glycoproteins is catalyzed by α1–6 fucosyltransferase (FucT8), which transfers an L-fucose residue to the reducing terminal *N*-acetylglucosamine on *N*-glycans via an α1–6-linkage (2). This oligosaccharide structure can be detected by lectin affinity electrophoresis using *Lens culinaris* agglutinin (LCA), which has an affinity to core-fucosylated mono- and bi-antennary *N*-glycans (3–5). Therefore, the detection of AFP-L3 by this method has been clinically used to make a differential diagnosis of HCC from liver cirrhosis (6–8). LCA can be used for affinity chromatography, but using it for lectin blot analysis to evaluate cellular fucosylation can be difficult because of its low sugar binding specificity. Conventionally, in addition to LCA, other commercially available core fucose-binding lectins, such as *Pisum sativum* agglutinin (9), *Aleuria aurantia* lectin (AAL) (10–13), *Narcissus pseudonarcissus* agglutinin, *Vicia faba* agglutinin (14–16), and *Aspergillus oryzae* lectin (12, 17, 18) have been used in studies on glycobiology. However, most fucose-binding lectins recognize any type of fucosylation, and LCA binds not only to fucose but also to mannose residues in *N*-glycans (3).

A. oryzae lectin has been reported to be α1–6 fucose-specific but in fact also binds α1–2 fucose residues in lectin microarrays and in lectin frontal chromatography (12). Therefore, there is a

[S] This article contains supplemental Fig. S1–S5.

[1] To whom correspondence may be addressed. Tel.: 81-45-852-4001; Fax: 81-45-852-6357; E-mail: yuka.kobayashi@j-oil.com.
[2] To whom correspondence may be addressed. Tel.: and Fax: 81-54-238-4885; E-mail: achkawa@ipc.shizuoka.ac.jp.

[3] The abbreviations used are: HCC, hepatocellular carcinoma; PhoSL, *P. squarrosa* lectin; LCA, *Lens culinaris* agglutinin; AAL, *A. aurantia* lectin; RSL, *R. stolonifer* lectin; PA, pyridylaminated; FAC, frontal affinity chromatography; AFP, α-fetoprotein; *AFP-L3*, α1–6-fucosylated fetoprotein; Bt, effective ligand constant based on concentration dependence analysis.

real need for novel α1–6 fucose-binding lectins with a strict binding specificity.

In the course of our continued screening for new mushroom lectins (20, 21),[4] we found lectin activity for core fucose in the extracts of the mushroom *Pholiota squarrosa* and succeeded in the purification of a core fucose-binding lectin from the mushroom. Here, we describe the isolation, characterization, and biological activity of this core fucose-binding lectin.

EXPERIMENTAL PROCEDURES

Materials—Fruiting bodies of *P. squarrosa* were collected from Tochigi, Fukushima, and Miyagi prefectures, Japan, and identified by HyphaGenesis Inc. (MEX-1083). The fruiting bodies were frozen upon collection and stored at −20 °C. DEAE-Sepharose Fast Flow was purchased from GE Healthcare. Butyl-Toyopearl and TSK-GEL G3000SWXL were purchased from Tosoh (Tokyo, Japan). MALDI-TOF mass spectra were acquired on an AutoFlex mass spectrometer (Bruker Daltonics Inc., Billerica, MA). Erythrocytes were products of Nippon Biotest Laboratories Inc. (Tokyo, Japan) and Biotest AG (Dreieich, Germany). All of the sugars and glycoproteins used for the hemagglutinating inhibition tests and ELISA were purchased from Nacalai Tesque (Kyoto, Japan), Wako Pure Chemical Industries, Ltd. (Ōsaka, Japan), Calbiochem, and Sigma. Pyridylaminated (PA) oligosaccharides for frontal affinity chromatography (FAC) analysis were purchased from Takara Bio Inc. (Shiga, Japan) and Masuda Chemical Industries Co., Ltd. (Kagawa, Japan). HiTrap NHS-activated Sepharose was purchased from GE Healthcare. Stainless steel empty miniature columns (inner diameter, 2 mm; length, 10 mm; bed volume, 31.4 μl) were obtained from Shimadzu Co. (Kyoto, Japan). The Huh-7D12 cell line was purchased from DS Pharma Biomedical Co., Ltd. (Osaka, Japan). AFP from human cord serum was a product of SCIPAC Ltd. (Sittingbourne, UK). *N*-Glycosidase F was purchased from Roche Applied Science. Human serum samples for the study were prepared by KAC Co., Ltd. (Kyoto, Japan) with informed consent from the patients. The *L. culinaris* agglutinin lectin affinity HPLC column (LA-LCA, 0.46 × 15 cm), biotinylated LCA, and biotinylated AAL were products of J-Oil mills, Inc. (Tokyo, Japan).

Preparation of Affinity Adsorbent—Thyroglobulin and anti-human AFP antibody NB-011 (Nippon Biotest Laboratory, Inc.) were conjugated to HiTrap NHS-activated Sepharose according to the manufacturer's protocols.

Purification of PhoSL—All of the procedures were carried out at 4 °C. After defrosting, the fruiting bodies of *P. squarrosa* were homogenized and then extracted overnight with 10 mM Tris-HCl buffer (pH 7.2) containing 0.1% (v/v) sodium sulfite. The homogenate was centrifuged at 8500 × *g* for 20 min, and the resultant supernatant was applied to a DEAE-Sepharose column (2.5 × 5 cm) equilibrated with the same buffer. After unbound materials were washed with the buffer, the bound fraction was desorbed with a linear gradient elution of NaCl (0, 0.05, 0.1, 0.2, 0.5, and 1 M) in the same buffer. The lectin-containing fraction eluted with 0.2 M NaCl was concentrated by ultrafiltration and lyophilized. The lyophilized fraction was redissolved in PBS and applied to a column of thyroglobulin-agarose (2.5 × 15 cm) equilibrated with PBS. The column was exhaustively washed with the same buffer, and the adsorbed lectin was desorbed with 0.2 M ammonia. The eluate was immediately neutralized with 1 M HCl, dialyzed extensively against distilled water, and lyophilized. Approximately 2.7 mg of PhoSL was obtained from 100 g of the fresh fruiting bodies.

SDS-PAGE—SDS-PAGE (PhastGel Gradient 10–15 and Highdensity) was performed according to the method of Laemmli (22). Samples were heated in the presence or absence of 2-mercaptoethanol for 5 min at 100 °C. Gels were stained with Coomassie Brilliant Blue. The molecular mass standards, XL-Ladder Broad (APRO life Science Institute, Inc., Tokushima, Japan) and smart peptide protein standard (GenScript USA Inc. Piscataway, NJ), were used. Gels were also stained with Glycoprotein Staining kit and GelCode Phosphoprotein Staining kit (Thermo Fisher Scientific Inc., Waltham, MA) for glycosylated and phosphorylated proteins, respectively.

Gel Filtration for Estimation of Molecular Mass—Gel filtration by HPLC was carried out on a TSK-gel G3000SWXL column (7.8 × 300 mm) at 25 °C in 20 mM phosphate buffer (pH 7.4) containing 20% acetonitrile at a flow rate of 0.5 ml/min. Fractions were collected by monitoring the absorbance at 280 nm. The molecular mass was calibrated with standard proteins (Sigma).

Isoelectric Focusing—Isoelectric focusing was performed on a PhastGel IEF gel (pH 3–9) using Phastsystem (GE Healthcare). The pI standards were purchased from GE Healthcare.

N-terminal Sequence Analysis—The N-terminal amino acid of the intact protein was analyzed on a PPSQ-21A protein peptide sequencer (Shimadzu).

Bioinformatics Analysis—A sequence homology search was performed using the BLAST program (www.ncbi.nlm.nih.gov).

Peptide Synthesis—A peptide possessing the sequence determined by N-terminal sequence analysis (NH_2-APVPVTKLVCD-GDTYKCTAYLDFGDGRWVAQWDTNVFHTG-OH) was synthesized chemically by Toray Research Center (Tokyo, Japan). The crude synthesized peptide was purified by reverse-phase HPLC using an ODS column (Wakosil-II 5C18HG, 2 × 25 cm) (Wako Pure Chemical Industries) with a linear gradient of 10–90% CH_3CN, 0.05% trifluoroacetic acid in H_2O at a flow rate of 1 ml/min. The effluent was monitored at 215 nm. The solvent was removed by evaporation at room temperature, leaving behind the peptide as a residual powder.

Thermostability, pH Stability, and Metal Cation Requirements—The thermostability and pH stability of the lectin were examined as described previously (23–26). Briefly, samples in PBS (0.1 mg/ml) were heated for 30 min at 4, 30, 40, 50, 60, 70, 80, or 100 °C, cooled on ice, and titrated. In addition, the samples in PBS were heated for 0.5, 1, 2, 3, 6, or 12 h at 4, 60, 80, or 100 °C, cooled on ice, and titrated. The pH stability of the lectin was measured by incubating the samples in different buffers (0.1 mg/ml) for 12 h at 4 °C, dialyzed against PBS, and titrated in PBS. The following buffers were used: 50 mM glycine-HCl buffer (pH 2.0, 3.0), 50 mM sodium acetate buffer (pH 4.0, 5.0), 50 mM sodium phosphate buffer (pH 6.0, 7.0), 50 mM Tris-HCl buffer (pH 8.0), and 50 mM glycine-NaOH buffer (pH 9.0–11.0). To examine the metal cation requirements for hemagglutina-

[4] Y. Kobayashi and H. Kawagishi, unpublished data.

tion by the lectin, the sample (0.1 mg/ml) was incubated in 10 mM EDTA for 1 h at room temperature, dialyzed against PBS, and titrated. Afterward, 0.1 M metal cation ($CaCl_2$, $FeCl_2$, $MgCl_2$, $MnCl_2$, or $ZnCl_2$) was added to the demetalized lectin, and the solution was incubated for 1 h at room temperature and titrated.

Solubility—The solubility of the lectins, PhoSL and LCA, was measured by incubating each sample in various buffers (1 mg/ml) for 12 h at 4 °C, monitoring absorbance at 280 nm, and titrating in PBS. The following buffers were used: PBS, 10 mM Tris-HCl buffer (pH 7.4), 10 mM sodium phosphate buffer (pH 7.4), 10 mM potassium phosphate buffer (pH 7.4), 10 mM sodium citrate buffer (pH 7.4), and 50 mM Veronal buffer (pH 8.6).

Hemagglutination and Inhibition Assay—The hemagglutinating activity of lectin was determined using a 2-fold serial dilution procedure using intact erythrocytes. Briefly, 20 μl of a lectin-containing solution was added to the far left wells of a 96-well microtiter plate with U-shaped wells (Greiner), and a 2-fold serial dilution in PBS was made down the plate. Thereafter, 20 μl of a 3% solution of erythrocytes was added to each well, and hemagglutination was allowed to proceed for 1 h at room temperature. The hemagglutination titer was determined as the reciprocal of the highest dilution in which hemagglutination was observed. Results were interpreted as follows: tight button = negative; spread red blood cells = positive.

Inhibition was expressed as the minimum concentration of each sugar or glycoprotein required to inhibit hemagglutination of titer 4 of the lectin using rabbit erythrocytes. Briefly, 10 μl concentrations of each sugar- or glycoprotein-containing solution was added to the wells of a 96-well microtiter plate with U-shaped wells (Greiner), and a 2-fold serial dilution in PBS was made down the plate. Next, 10 μl of titer 4 of the lectin dissolved in PBS was added to each well, and the reaction was allowed to proceed for 1 h at room temperature. 20 μl of a 3% solution of erythrocytes was added to each well, and hemagglutination was allowed to proceed for 1 h at room temperature. The hemagglutination inhibitory concentration of each sugar was expressed as the reciprocal of the highest dilution in which inhibition of hemagglutination was observed.

FAC Analysis—The principle and protocol of FAC analysis have been described previously (27–29). Briefly, the lectin and the peptide were each dissolved in 0.2 M $NaHCO_3$ containing 0.5 M NaCl (pH 8.3) and coupled to a HiTrap *N*-hydroxysuccinimide-activated Sepharose. After washing and deactivation of excess active groups by 0.5 M Tris containing 0.5 M NaCl (pH 8.3), the lectin- or peptide-immobilized Sepharose beads were suspended in 10 mM Tris-HCl buffer (pH 7.4) containing 0.8% NaCl (TBS); the slurry was packed into a stainless steel column (2.0 × 10 mm) and connected to the FAC-1 machine that had been specially designed and manufactured by Shimadzu. The amount of immobilized protein was determined by measuring the amount of uncoupled protein in the washing solutions by the method of Bradford (30). The flow rate and the column temperature were kept at 125 μl/min and 25 °C, respectively. After equilibration with TBS, an excess volume (0.3 ml) of PA-glycans (3.8 or 4.5 nM) was successively injected into the columns by an autosampling system. Elution of PA-glycans was monitored by measuring fluorescence (excitation and emission wavelengths, 310 and 380 nm, respectively). The elution front relative to that of a standard oligosaccharide (PA-05, Manα1-3(Manα1-6)Manβ1-4GlcNAcβ1-4GlcNAc-PA), *i.e.* $V - V_0$, was then determined. V is the elution volume of each PA sugar. PA-05, which has no affinity to the lectin, was used for the determination of V_0. For obtaining the effective ligand content (Bt) of each lectin column, concentration dependence analysis was performed using varying concentrations (0.5–10 μM) of PA402 (Masuda Chemicals, Takamatsu, Japan). Woolf-Hofstee plots were made using the $V - V_0$ values, and the Bt values were thus obtained. Next, using the Bt values for each lectin column, K_d values for a series of glycans were calculated from the equation $K_d = Bt/(V - V_0)$, if $K_d \gg [A]_0$. In this study binding affinity is discussed using an association constant (K_a), where K_a is the inverse of K_d ($K_a = 1/K_d$).

Cell Culture and Purification of AFP-L3—Huh7 cells were cultured in Dulbecco's modified Eagle's medium (Sigma) containing 10% fetal bovine serum (Invitrogen) and 1/100 penicillin-streptomycin solution (×100) (Wako Pure Chemical Industries) at 37 °C and 5% CO_2. The cultured supernatant was centrifuged at 8500 × *g* for 20 min and filtered. The resultant supernatant was applied to a column of anti-human AFP antibody NB-011 (Nippon Biotest Laboratories)-immobilized Sepharose (5 ml) equilibrated with PBS. After unbound materials were washed with the buffer, the bound fraction was desorbed with 0.1 M glycine-HCl buffer (pH 3.0). The eluant was immediately neutralized with 1 M Tris-HCl (pH 9.0). The fractions were concentrated and applied to an LA-LCA column (0.46 × 15 cm) equilibrated with 50 mM Tris-H_2SO_4 (pH 7.2). The column was exhaustively washed with the same buffer, and the adsorbed AFP was eluted by a linear gradient of methyl α-mannoside (0 to 0.2 M) in the buffer. The eluant was dialyzed extensively against distilled water, ultrafiltered, and concentrated.

Deglycosylation of the Anti-human AFP Antibody—Anti-human AFP antibody NB-011 (150 μg) was incubated with 25 units of *N*-glycosidase F (Roche Applied Science) in a total volume of 1 ml of glycosidase reaction buffer (20 mM sodium phosphate buffer (pH 7.4)) containing 0.5% *n*-octyl glucoside (Dojindo Laboratories, Kumamoto, Japan) for 24 h at 37 °C. The deglycosylated antibody was stored in aliquots at 4 °C with 0.1% sodium azide (31).

Biotinylation of Lectin—PhoSL was incubated with biotin amidocaproate *N*-hydroxysuccinimide ester (Sigma) in 0.1 M $NaHCO_3$ with haptenic sugar for 12 h at 4 °C and then desalted with Sephadex G-25 columns (GE Healthcare).

ELISA—Interaction between glycosylated proteins and L-Fuc-specific lectins was detected by ELISA. Ninety-six-well ELISA plates (Greiner Bio-One, Frickenhausen, Germany) were coated by adding 25 μl of each diluted protein or glycoprotein (100 ng/ml) in 0.1 M carbonate buffer (pH 9.5) per well, and the plates were then incubated overnight at 4 °C. Subsequently, the plates were blocked with PBS containing 1% bovine serum albumin (BSA) for 1.5 h at room temperature and then rinsed with wash buffer (PBS containing 0.05% Tween 20, pH 7.4) 3 times before the addition of each biotinylated lectin in blocking buffer (1 μg/ml). After incubation for 1 h at room temperature, the plates were washed 3 times before the addi-

tion of horseradish peroxidase-streptavidin (Vector Laboratories Inc., Burlingame, CA). After the plates were washed, 3,3′,5,5′-tetramethylbenzine microwell peroxidase substrate system (KPL) was used for colorimetric analysis, and the absorbance was measured at 450 nm.

Human Serum Samples Information—Human serum samples for the study were prepared by KAC Co., Ltd., with informed consent from the patients. The normal volunteers were NV-1 (sample ID S018282, female, age 41), NV-2 (sample ID S01828, male, age 46), and NV-3 (sample ID S018290, male, age 29). The HCC patients were HCC-1 (sample ID S09119, male, age 71, Grade 00, TNM T3NxM0, Stage III, CEA 2.3, AFP 6.9), HCC-2 (sample ID S09069, male, age 44, Grade G3, TNM T1N0M0, Stage N/A, CEA N/A, AFP 956.31), and HCC-3 (sample ID S09227, male, age 50, Grade G2, TNM T3N0M0, Stage III, CEA 0.606, AFP 10.66). Human serum samples were pretreated with Proteome Purify™ 12 (R&D Systems, Inc. Minneapolis, MN).

Antibody-Lectin Sandwich Assay—Ninety-six-well ELISA plates were coated by adding 25 μl of diluted deglycosylated antibody in 0.1 M carbonate buffer (pH 9.5) per well, and the plates were then incubated overnight at 4 °C. The next day the plates were blocked for 1.5 h at room temperature with 150 μl of blocking buffer (PBS containing 1% BSA) and then rinsed with wash buffer (PBS containing 0.05% Tween 20, pH 7.4) 3 times. Each sample in the blocking buffer or the human serum samples was allowed to react for 1.5 h at 37 °C, and the plates were washed 3 times before the addition of each lectin in the blocking buffer (1 μg/ml). After incubation for 1 h at room temperature, the plates were washed 3 times before the addition of horseradish peroxidase-streptavidin. After the plates were washed, 3,3′,5,5′-tetramethylbenzine microwell peroxidase substrate system was used for colorimetric analysis, and the absorbance was measured at 450 nm.

Human Colon Cancer Array Analysis—Human colon cancer array slides carrying primary or metastatic colon cancers were obtained from KURABO Industries Ltd. (Osaka, Japan). In total, 124 colon cancer tissues, including 79 primary and 45 metastatic cancer tissues and 11 normal colon tissues, were subjected to immunohistochemical analysis. Tissue microarray slides were deparaffinized with xylene and ethanol. The slides were pretreated with avidin/biotin solution and then with peroxidase blocking reagent (DAKO, Carpinteria, CA). After washing twice with PBS, the slides were incubated in TBST (10 mM Tris-HCl buffer (pH 7.4) containing 0.8% NaCl and 0.05% Tween 20) containing 5% BSA at 4 °C overnight. Next, the slides were incubated with biotinylated AAL (5.0 μg/ml) or PhoSL (50 μg/ml) for 1 h at room temperature. The slides were then washed 3 times with PBS and incubated with the ABC kit (Vector Laboratories) for 30 min at room temperature. After washing 3 times with PBS, positive staining was visualized using diaminobenzidine (DAKO). Statistical analysis was performed using the χ^2 test.

RESULTS

Isolation and Molecular Properties of PhoSL—A lectin was purified from extracts of fruiting bodies of *P. squarrosa* using DEAE-Sepharose and affinity chromatography on thyroglobulin-agarose. Because very little of the lectin activity was recovered from the affinity support (the thyroglobulin-agarose) by elution with the haptenic sugar, L-fucose, even at a concentration of 0.2 M, the lectin was eluted with 0.2 M ammonia. The purified lectin, designated as PhoSL, gave a band with a mass of 4.5 kDa on SDS-PAGE in the presence (Fig. 1*A*, *lane 1*, and *B*, *lane 1*) and two bands with masses of 4.5 and 14 kDa in the absence of 2-mercaptoethanol (Fig. 1*B*, *lane 2*). Isoelectric focusing gave a band near p*I* 4.0 (Fig. 1*C*). The use of assay kits for the detection of glycoproteins and phosphoproteins showed no significant bands on the membrane, suggesting that very low or undetectable levels of glycosylation and phosphorylation were present in the protein (data not shown). MALDI-TOF mass analysis of PhoSL yielded molecular ions from *m/z* 4,229 to 4,455 and small peaks at *m/z* 8,932 and 13,373 (data not shown). HPLC gel filtration of the intact lectin gave a peak at an elution volume corresponding to a molecular mass of 14 kDa (supplemental Fig. S2).

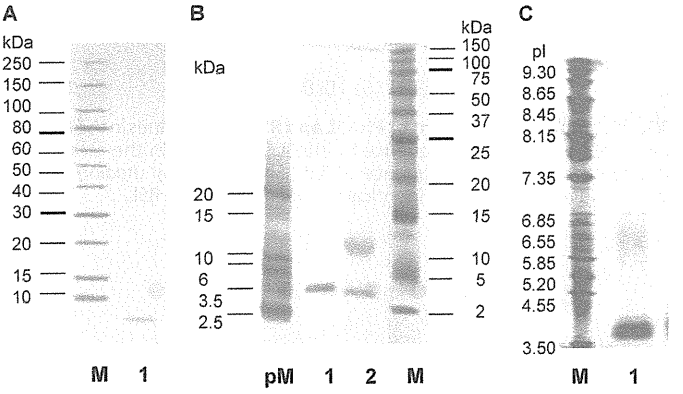

FIGURE 1. **Characterization of PhoSL.** *A*, shown is an SDS-PAGE linear gradient gel (10–15%). *Lane M* indicates marker proteins; *lane 1*, purified PhoSL under reducing conditions with 2-mercaptoethanol. *B*, shown is a high density SDS-PAGE gel. *Lane pM* indicates marker peptides; *lane 1*, purified PhoSL under reducing conditions with 2-mercaptoethanol; *lane 2*, purified PhoSL non-reduced; *lane M*, marker proteins. *C*, shown is isoelectric focusing of PhoSL. *Lane M* indicates marker proteins; *lane 1*, PhoSL.

N-terminal Amino Acid Sequence Analysis—N-terminal amino acid sequence analysis of PhoSL gave the 40-amino acid sequence NH_2-APVPVTKLVCDGDTYKCTAYLDFGDGRW-VAQWDTNVFHTG-OH (Fig. 2). The amino acid sequence of PhoSL was analyzed by the BLAST program, and the sequence showed homology to a lectin from *Rhizopus stolonifer* (RSL) (85%) (Fig. 2).

Stability of PhoSL—The lectin activity of PhoSL was extraordinarily stable over a wide range of temperatures between 4 and 100 °C at an incubation time of 30 min (Fig. 3*A*). The activity was also retained at 60 °C for 12 h and at 80 °C for 6 h (Fig. 3*B*). Half of the lectin activity was maintained even at 100 °C for 3 h (Fig. 3*B*). Similarly, the lectin activity was very stable over the wide range of tested pH values (pH 2.0–11.0) (Fig. 3*C*). Treatment with EDTA or the addition of the metal cations $CaCl_2$, $FeCl_2$, $MgCl_2$, $MnCl_2$, or $ZnCl_2$ did not produce any changes in the lectin activity. This result indicates that the lectin does not require metal ions for binding (date not shown). PhoSL was soluble in all the buffers used; however, LCA was soluble in 10 mM Tris-HCl buffer (pH 7.4), 10 mM sodium phosphate buffer (pH 7.4), and 50 mM Veronal buffer (pH 8.6) but not soluble in